

# *In Vivo* Anti-Biofilm and Anti-Bacterial Non-Leachable Coating Thermally Polymerized on Cylindrical Catheter

Chao Zhou, ‡<sup>1,2</sup> Yang Wu, ‡<sup>1,2</sup> Kishore Reddy Venkata Thappeta, ‡<sup>3</sup> Jo Thy Lachumy Subramanian,<sup>1,2</sup> Dicky Pranantyo,<sup>4</sup> ET Kang,<sup>4</sup> Hongwei Duan<sup>1,2</sup>, Kimberly Kline,<sup>2,3</sup> Mary B. Chan-Park\*<sup>1,2</sup>

<sup>1.</sup> *School of Chemical and Biomedical Engineering, Nanyang Technological University (NTU), 62 Nanyang Drive, Singapore 637459.*

<sup>2.</sup> *NTU, Centre for Antimicrobial Bioengineering.*

<sup>3.</sup> *Singapore Centre for Environmental Life Science Engineering (SCELSE), School of Biological Sciences, Nanyang Technological University, Singapore.*

<sup>4.</sup> *National University of Singapore, Department of Chemical and Biomolecular Engineering, Singapore*

*‡ These authors contribute equally.*

**ABSTRACT** Catheters are indispensable tools of modern medicine but catheter-associated infection is a significant clinical problem, even when stringent sterile protocols are observed. When the bacteria colonize catheter surfaces, they tend to form biofilms making them hard to treat with conventional antibiotics. Hence, there is a great need for inherently antifouling and anti-bacterial catheters that prevent bacterial colonization. This paper reports the preparation of non-leachable anti-biofilm and anti-bacterial cationic film coatings directly polymerized from actual tubular silicone catheter surfaces *via* the technique of supplemental activator and reducing agent surface initiated atom transfer radical polymerization (SARA SI-ATRP). Three crosslinked cationic coatings containing (3-acrylamidopropyl) trimethyl-ammonium chloride (AMPTMA), or quaternized polyethylenimine methacrylate (Q-PEI-MA) together with a crosslinker (polyethylene glycol dimethacrylate, PEGDMA) were tested. The *in vivo* anti-bacterial and anti-biofilm effect of these non-leachable covalently linked coatings (using a mouse catheter model) can be tuned to achieve 1.95 log (98.88%) reduction and 1.26 log (94.51%) reduction of clinically relevant pathogenic bacteria (specifically with Methicillin-resistant *Staphylococcus aureus* (MRSA) and Vancomycin -resistant *Enterococcus faecalis* (VRE)). Our good *in vivo* bactericidal killing results using the murine catheter-associated urinary tract infection (CAUTI) model show that SARA SI-ATRP grafting-from technique is a viable technique for making non-leachable antibiofilm coating even on “small” (0.30/0.64 mm inner/outer diameter) catheter.

**KEYWORDS** SARA SI-ATRP; anti-biofilm; anti-bacterial; non-leachable coating; catheter

## 1. Introduction

Indwelling catheters, such as Foley catheters, urinary catheters, central venous catheters (CVCs), peripherally inserted central catheters (PICCs), cerebrospinal fluid shunts or continuous

ambulatory peritoneal dialysis catheters,<sup>1</sup> are indispensable in modern medicine. However, infections due to these catheters are not uncommon and cannot be totally eradicated even with the most sterile hospital implantation environment. In the USA alone, 5% of the 5 million CVCs lead to bloodstream infections.<sup>2</sup> These nosocomial infections such as catheter-related bloodstream infection (CRBSI) or catheter-associated urinary tract infection (CAUTI),<sup>3</sup> may lead to substantial mortality (of up to 25%).<sup>4</sup> Bacteria usually colonize these devices as biofilms, which are thick extracellular polymer layers that protect the community of bacteria from antibiotics and the host immune system; the effectiveness of antibiotics towards biofilm bacteria is usually 10x to 1000x less than that towards planktonic bacteria.<sup>1, 5</sup> Further, bacteria are prone to resistance to antibiotics and the prolonged use of antibiotics in catheters designed with controlled release of antibiotics is generally discouraged.

Three main classes of coatings have been employed for reducing bacterial infection of indwelling catheters, but the efficacy seems to be still unsatisfactory.<sup>2, 6</sup> The first class of coating involves the use of controlled release of leachable antiseptics such as chlorhexidine,<sup>7-8</sup> but the toxicity limits their application. Leaching of silver alloy coating has also been extensively exploited but there have been conflicting results about its efficacy.<sup>9-10</sup> In a study published in *The Lancet*, Pickard *et al.* established that silver alloy- and nitrofurantoin-coated catheters do not reduce the likelihood of CAUTI.<sup>9</sup> The second and third categories involve non-fouling coatings and contact-active coatings respectively,<sup>11-12</sup> but these are typically not anti-biofilm. Hydrophilic coatings are known to be non-fouling and when combined with cationicity, they can become antimicrobial.<sup>13-18</sup> Various kinds of hydrophilic or cationic polymers, such as poly(ethylene glycol) (PEG),<sup>19-20</sup> poly(acrylic acid) (PAA),<sup>21</sup> poly(acrylamide) (PAAm),<sup>22</sup> poly([2-(methacryloyloxy)ethyl] dimethyl (3-sulfopropyl) ammonium),<sup>23</sup> poly((2-(methacryloyloxy)-ethyl) dimethyl-(3-sulfopropyl)-ammonium

hydroxide) (P(DMAPS))<sup>19</sup> and ethylcellulose<sup>24</sup> have been incorporated onto surfaces by UV-initiated grafting or plasma treatment.

Non-fouling coating inhibits protein or cells adsorption but do not kill any bacteria adsorbed so that with prolonged use, bacteria will eventually deposit on any surface since they are much bigger (around 1  $\mu\text{m}$ ) than proteins. Anti-bacterial contact-active coatings are usually cationic but they will usually adsorb proteins and bacteria cells since these are anionic. Either of the two latter classes of coatings by themselves are non-antibiofilm which requires the simultaneous prevention of protein adsorption and bacterial killing. Thus far, most reported coatings are either anti-fouling or contact-killing but not anti-biofilm.<sup>25-26</sup> In most reports, the testing protocols involve only buffer rather than biofilm stimulating medium which can more closely simulate the clinical catheter use situation or biofilm mouse models. There are very few reports on anti-biofilm coatings which involve the prevention of biofilm formation on catheter. There are even fewer reports on *in vivo* anti-biofilm coatings, which biofilm forms on catheter surfaces through initial attachment and then maturation of bacteria. We hypothesized that we should have a coating that is both non-fouling and anti-bacterial.

To our knowledge, there are no reports on *in vivo* studies with actual tubular catheter surfaces coated with hydrophilic anti-bacterial and anti-biofilm polymers for resisting colonization by difficult-to-treat bacteria such as Methicillin-resistant *Staphylococcus aureus* (MRSA) or Vancomycin-resistant *Enterococcus faecalis* (VRE). We have developed a method, using thermal initiated radical polymerization, for forming anti-biofilm coatings on long slender PDMS tubular catheter that avoids uneven coating associated with UV or argon plasma activation. The 3-step procedure for the covalent grafting of anti-bacterial and anti-biofilm films on PDMS tubular catheter is illustrated schematically in Scheme 1. Firstly, a multifunctional biomimetic layer of

polydopamine (PDA) is deposited on the PDMS catheter (Step 1, Scheme 1). Subsequently, the ATRP initiator ( $\alpha$ -bromoisobutyryl bromide, BiBB) is immobilized onto the hydroxyl and amino groups present on the PDA (step 2).<sup>27-28</sup> Then, the cationic and the uncharged monomers/crosslinker are heated in air-free solvent (Step 3) so that they polymerize from the surface-immobilized BiBB initiator *via* SARA SI-ATRP. We prepared three anti-bacterial coatings (Table 1) containing (3-acrylamidopropyl) trimethylammonium chloride (AMPTMA), poly(ethylene glycol) dimethacrylate (PEGDMA), quaternized polyethylenimine methacrylate (Q-PEI-MA) as monomers or crosslinkers on PDMS catheter surface. The anti-bacterial and anti-biofilm effect of the films coated onto PDMS tubular catheters were evaluated *via in vitro* and *in vivo* assays, as well as *via* X-ray photoelectron spectroscopy (XPS), contact angle measurement, field emission-scanning electron microscopy (FE-SEM), atomic force microscopy (AFM) and cytocompatibility and hemolytic assays.

## 2. Experimental

### 2.1 Materials

(3-acrylamidopropyl) trimethylammonium chloride (AMPTMA, 75%), poly (ethylene glycol) dimethacrylate (PEGDMA,  $M_n=750$ ), branched polyethylenimine (PEI,  $M_n=800$ ), glycidyl methacrylate (97%), 2-Hydroxyethyl methacrylate (HEMA, 99%), bromoethane (99%), triethylamine (TEA, 99%), dopamine hydrochloride (DA),  $\alpha$ -bromoisobutyryl bromide (BiBB, 98%), CuBr (97%), Tris base (Trizma base, Pharma Grade), 4-dimethylaminopyridine (DMAP, 99%), ethyl acetate (anhydrous, 99.8%), methanol (99.8%), diethyl ether (99.5%), ethanol (99.8%), ethylenediaminetetraacetic acid disodium salt solution (0.2 M), N,N,N',N'',N''-pentamethyldiethylenetriamine (PMDETA, 99%), phosphate buffer saline (tablets), D-(+)-glucose

(99.5%), dimethyl sulfoxide (DMSO, for molecular biology), Triton X-100 (for molecular biology) and glutaraldehyde solution (25% in H<sub>2</sub>O) were purchased from Sigma-Aldrich. High purity deionized water with a resistivity of >15MΩ cm was obtained from a Merck Millipore Integral 3 water purification system. Polydimethylsiloxane (PDMS) catheter (0.30 mm/0.64 mm ID/OD) was purchased from Braintree Scientific. PDMS films were prepared from Foley catheter tubes (2.60/5.33 mm ID/OD) purchased from Liberty Medica, and cut into halves along the longitudinal axis. Catheters were washed with water/ethanol, then sonicated and dried before use. Copper wire (Cu (0), d= 1 mm) was washed with HCl, rinsed with methanol and dried under a stream of nitrogen gas before use. LIVE/DEAD® BacLight™ bacterial viability kit (L13152) was purchased from Thermo Fisher Scientific. 3-[4, 5-dimethylthiazoyl-2-yl]-2, 5-diphenyl tetrazolium bromide (MTT) was purchased from Alfa Aesar.

Bacteria strains including *Escherichia coli* 8739 (EC, ATCC 8739) and *Staphylococcus aureus* 29213 (SA, ATCC 29213) were bought from American Type Culture Collection (ATCC). *Pseudomonas aeruginosa* O1 (PAO1, ATCC 15692), vancomycin-resistant *Enterococci faecalis* V583 (VRE, ATCC 700802), and methicillin-resistant *Staphylococcus aureus* CPS22 (MRSA, ATCC BAA-40) were kindly provided by Kimberly Kline's lab, which bought them from ATCC. Mueller Hinton Broth medium (MHB), Brain Heart Infusion medium (BHI), Tryptic Soy Broth medium (TSB) and Lysogeny Broth Agar medium (LB Agar) were purchased from BD Difco. All media and PBS buffer (10mM, PH 7.4) were prepared in DI water according to the supplier's instructions and were autoclaved before use. 3T3 fibroblast cells (ATCC CRL-1658) were bought from ATCC. Dulbecco's Modified Eagle Medium (DMEM) high glucose with L-glutamine, Fetal Bovine Serum (FBS), Penicillin-Streptomycin (100×) and trypsin-EDTA (0.25%) were bought from Thermo Fisher Scientific. Six to seven weeks old female wild-type C57BL/6 mice, purchased

from In Vivos Pte Ltd, Singapore, were used for *in vivo* biofilm studies. Infections were carried out after 1 week of adaptation in the animal facility house after delivery, as previously described.<sup>29</sup> All studies and procedures were approved by the Animal Studies Committee at Nanyang Technological University.

## 2.2 Synthesis of Quaternized polyethylenimine methacrylate (Q-PEI-MA)

Branched polyethylenimine (PEI 10 g, 12.5 mmol) was dissolved in 20 ml ethanol and the solution was cooled to 0 °C. A cold solution of glycidyl methacrylate (5.33 g, 37.5 mmol) in 10 ml ethanol was added dropwise to the PEI solution over a period of 30 minutes and stirred for 24 hours at room temperature. Subsequently, a cold solution consisting of 30 ml of bromoethane mixed with 10 ml of ethanol was added dropwise into the above solution and stirred for 24 hours at room temperature. After the reaction, ethanol was removed with a rotary evaporator operated under vacuum and the resulting product was precipitated in diethylether. Lastly, the product was dried overnight in a vacuum dryer at room temperature to produce a yellow powder (yield 91%). The <sup>1</sup>H NMR spectrum is shown in Figure S1. (<sup>1</sup>H NMR (300 MHz, D<sub>2</sub>O, δ, ppm): 6.12 (d, 1 H, CH<sub>2</sub>=C(CH<sub>3</sub>)), 5.67 (s, 1 H, CH<sub>2</sub>=C(CH<sub>3</sub>)), 5.24 (d, 4 H, -NH<sub>2</sub>), 5.06 (m, 4 H, -O-CH<sub>2</sub>-), 4.02 (s, 4 H, -CH-OH), 3.9-2.3 (dddd, 268 H, -CH<sub>2</sub>-CH<sub>2</sub>-NH-), 1.85 (t, 15 H, -CH<sub>3</sub>), 1.13 (m, 85 H, N<sup>+</sup>H-CH<sub>3</sub>).

## 2.3 Preparation of PDMS catheter surface initiator

Dopamine hydrochloride (4 mg/ml) was first dissolved in 10 mM Tris-HCl (pH 8.5). Clean PDMS catheter tubes were cut into pieces 5 mm in length and were then immersed into the solution. The mixture was stirred for 72 hours until the PDMS catheter tubes showed an evident color change to dark brown. The tubes were then rinsed with ultrapure water and then with ethanol

to remove traces of polydopamine that were not attached onto the PDMS surface. The tubes were then dried overnight in a vacuum dryer at 50 °C.

In general, we used excess surface BiBB initiator and the surface density of BiBB initiator shall be called the control (or medium) density. The PDA coated PDMS catheter tubes were subsequently immersed in a solution consisting of 20 ml of anhydrous ethyl acetate, TEA (1.64 g, 16.2 mmol) and DMAP (1.00 g, 8.2 mmol). This solution was then purged with nitrogen gas for 30 minutes. A solution consisting of BiBB (3.72 g, 16.2 mmol) and 20 ml of ethyl acetate was added dropwise into the mixed solution over a period of 60 minutes at 0 °C. The resulting solution was then stirred at room temperature for 24 hours. Once the reaction was completed, the modified PDMS catheter tubes were washed with ethanol thrice and dried overnight in a vacuum dryer at room temperature.

We also prepared a low density coverage of BiBB surface initiator on PDMS catheter by following a similar procedure but with lesser TEA, DMAP and BiBB (now denoted as Step 2 (LD)); the PDA coated PDMS catheter tubes were subsequently immersed in a solution consisting of 20 ml of anhydrous ethyl acetate, TEA (0.33 g, 3.24 mmol) and DMAP (0.20 g, 1.64 mmol). This solution was then purged with nitrogen gas for 30 minutes. A solution consisting of BiBB (0.74 g, 3.24 mmol) and 20 ml of ethyl acetate was added dropwise into the mixed solution over a period of 60 minutes at 0 °C. The resulting solution was then stirred at room temperature for 24 hours. Once the reaction was completed, the modified PDMS catheter tubes were washed with ethanol thrice and dried overnight in a vacuum dryer at room temperature.

We also prepared a high density BiBB coverage on the PDMS surface by the following protocol (denoted as Step 2 (HD)) by doing the BiBB grafting twice as follows (Scheme S2): (i) BiBB was

grafted on PDA and then ATRP of poly(HEMA) brush was performed. HEMA (5 ml, 41 mmol), CuBr (57.4 mg, 0.4 mmol), PMDETA (83.0  $\mu$ l, 0.4 mmol) and 25 BiBB/PDA-coated catheters were dissolved/suspended in 10 ml methanol; the solution was purged with nitrogen gas for 30 minutes and then sealed with a rubber stopper. The reaction was carried out at 50 °C for 24 hours with stirring. After reaction, the modified catheters were washed sequentially with EDTA- $\text{Na}_2$  solution, DI water, ethanol and DI water for 30 minutes each. Lastly, the catheter tubes were dried overnight in a vacuum drying oven at room temperature. (ii) Poly(HEMA) brush on the surface was reacted with BiBB and then further ATRP was performed. The catheters with poly(HEMA) brush were subsequently immersed in a solution consisting of 20 ml of anhydrous ethyl acetate, TEA (1.64 g, 16.2 mmol) and DMAP (1.00 g, 8.2 mmol). This solution was then purged with nitrogen gas for 30 minutes. A solution consisting of BiBB (3.72 g, 16.2 mmol) and 20 ml of ethyl acetate was added dropwise into the mixed solution over a period of 60 minutes at 0 °C. The resulting solution was then stirred at room temperature for 24 hours. Once the reaction was completed, the modified PDMS catheter tubes were washed with ethanol thrice and dried overnight in a vacuum dryer at room temperature.

#### **2.4 Preparation of coating 1 onto PDMS catheter by SARA SI-ATRP**

In a Schlenk flask, PDMS catheter tubes modified with surface initiators, AMPTMA (14.5 mmol, 3.99 g), PEGDMA (1.45 mmol, 1.089 g),  $\text{CuBr}_2$  (0.145 mmol, 32.4 mg) and PMDETA (0.145 mmol, 29.9  $\mu$ l) were dissolved in 10 ml of a 50/50 volume mixture of water and methanol. A magnetic stirring bar and copper wire (1 g,  $d = 1$  mm) were added to the flask, the solution was purged with nitrogen gas for 30 minutes and then sealed with a rubber stopper. The reaction was carried out at 50 °C for 24 hours with stirring. Once the reaction was completed, the coated catheter tubes were washed sequentially with EDTA- $\text{Na}_2$  solution, DI water, ethanol and DI water for 30

minutes each. Lastly, the catheter tubes were dried overnight in a vacuum drying oven at room temperature.

Coating 1 (low grafting density (LD)), coating 1 (High grafting density (HD)), coating 2 and coating 3 were prepared by similar procedures.

## **2.5 Characterization**

<sup>1</sup>H NMR spectra were obtained with an AVANCE 300 MHz spectrometer (Bruker, U.S.A), using the solvent signal for calibration. X-ray photoelectron spectroscopy (XPS) spectra were obtained using an ESCALABMK-II spectrometer (VG Scientific Ltd, West Sussex, Britain). A magnesium anode was used as Mg Ka X-ray source. Electrons emitted from the film surface were captured by an electron multiplier. Static water contact angles were measured using a FTA 200 goniometer (First Ten Ångstroms, USA) and employing the sessile drop method at room temperature. The topographies of the modified catheter surfaces were studied in the dry state by tapping mode AFM using a Dimension Icon microscope (Bruker, USA), catheter samples were cut into 3 mm × 3 mm films before characterization. The modified catheters were measured using Fourier-transform infrared spectrometer (FT-IR) with ATR accessory at an incident angle of 90° (Nicolet 5700, Thermo Fisher Scientific, U.S.A).

The surface morphologies of the modified and native PDMS catheters were studied with Field Emission Scanning Electron Microscopy (JEOL JSM-6701 F, Japan). The modified catheters were first coated with a platinum layer to provide surface conduction before scanning with FE-SEM. Olympus microscope (Model BX51) and Olympus DP71 camera were used for the live/dead bacteria imaging.

The surface charge on coated surface is characterized by surface zeta potential measurement *via* Anton Paar Electro Kinetic Analyzer. The coated PDMS slides are firstly cut into 4×2 cm pieces; and fixed onto the electrode. The coated slide is then rinsed with 0.01M KCl buffer with conductivity at 1239 mS/m of 120 s. The surface charge is then measured 4 times and the average value is reported.

## **2.6 Solution MIC test of catheter coating materials**

Overnight bacteria cultures were prepared in various media at 37 °C using Falcon round bottom polystyrene tubes and sub-cultured to mid-log phase for further use (MHB was used for EC, SA; BHI was used for VRE; TSB was used for PAO1 and MRSA). A series of sample solutions was prepared by two-fold dilution of 2000 mg/ml polymer stock in MHB to obtain final concentrations ranging from 1000 to 1 mg/ml. Then 100 µl of each diluted sample from the serial dilutions was added to a 96-well plate. Subsequently, 10<sup>6</sup> CFU/ml bacterial suspension was prepared in MHB from sub-cultured bacteria and added 100 µl to each well to form a final bacteria concentration of 5×10<sup>5</sup> CFU/ml. The 96-well plate was mixed on the plate shaker for 15 minutes and subsequently incubated statically at 37 °C for 16-18 hours. MIC is the lowest sample concentration which can inhibit bacteria growth by over 90%. The killing percentage was calculated by OD measurement compared with positive control (bacteria without sample treatment) and negative control (medium only). The test was repeated twice independently.

## **2.7 *In Vitro* Cytocompatibility Assay of catheters**

200 µl 10<sup>4</sup> cells/well 3T3 cells suspension in supplemented Dulbecco's Modified Eagle's Medium (DMEM with 10% FBS and 1% Penicillin-Streptomycin) were seeded in a 96 well cell culture plate and incubated for 24 hours at 37 °C in 5% CO<sub>2</sub>. At 24 hours, the medium was replaced,

catheter samples including the control sample (previously washed with water and ethanol and then dried) were placed into the wells and the plate was incubated for another 24 hours. At 48 hours, the catheter samples carefully removed with sterilized forceps. The medium was discarded and 100 µl of 3-(4,5-dimethylthiazol-2-yl)-2,5-diphenyltetrazolium bromide (MTT tetrazolium dye) in DMEM (1 mg/ml) was added to each well followed by another 4 hours of incubation. The MTT-DMEM solution was discarded and 100 µl dimethyl sulfoxide (DMSO) was added to each well. Absorbance values (ODs) were measured at 570 nm using a TECAN plate reader. Cell viability was calculated using Equation 1:

$$\text{Cell viability \%} = \frac{OD_{\text{sample well}}}{OD_{\text{control well}}} \times 100\% \quad (1)$$

## 2.8 Hemolytic Assays of catheters

Fresh human blood (5 ml) was collected from a healthy donor (age 25, male). Erythrocytes were separated by centrifugation at 1200 rpm for 10 minutes, washed thrice with PBS buffer and diluted to a final concentration of 5% v/v. Catheter samples including control sample were cut into 5 mm segments, washed with water/ethanol, and then dried in a vacuum oven before immersion into 100 µl erythrocytes stock placed in 96 well cell culture plate. All measurements were performed in triplicate. The plate was incubated at 37 °C for 1 hour with shaking at 150 rpm. Subsequently, the plate was centrifuged at 1500 rpm for 10 minutes. 50 µl aliquots of supernatant were transferred to a new 96 well plate and diluted with another 50 µl of PBS buffer. Hemolytic activity was determined by absorbance measurement at 540 nm with a TECAN Infinite® 200 PRO microplate reader. Triton X-100 (0.1% in PBS), which is able to lyse RBCs completely, was used as positive control while PBS buffer was used as negative control. The hemolysis percentage was calculated using the Equation 2:

$$\text{Hemolysis \%} = \frac{OD_{\text{sample}} - OD_{\text{negative}}}{OD_{\text{positive}} - OD_{\text{negative}}} \times 100\% \quad (2)$$

## 2.9 *In vitro* catheter biofilm test

Catheter samples including control sample were cut into 5 mm segments, washed with water & ethanol, and then dried before immersion into 200  $\mu\text{l}$  selected medium (BHI for VRE and TSB supplemented with 1% glucose for MRSA) in a 96 well plate.  $10^6$  CFU/ml bacteria suspension was made by diluting in 10 mM phosphate buffer saline (PBS, PH 7.4) from overnight culture; 8  $\mu\text{l}$  of this diluted bacteria suspension was added to each well. The plate was incubated at  $37^\circ\text{C}$  for 24 hours. Catheter samples were then removed and washed gently thrice with PBS buffer to remove unattached bacteria. Each catheter sample was then placed in an Eppendorf tube with 1 ml PBS buffer. The tube was placed in ultra-sonicator bath for 10-20 minutes and mixed by vortex for 5-10 minutes to strip and remove the attached biofilm from the surface. CFU number was counted by dilution of the stripped bacteria suspension in PBS and culture on Lysogeny Broth Agar (LB Agar) plate. Log reduction was calculated using the Equation 3:

$$\text{Number of log reduction} = \log_{10} \left[ \frac{CFU_{\text{control}}}{CFU_{\text{sample}}} \right] \quad (3)$$

## 2.10 Fluorescence Microscopy

Catheter samples including control samples were cut into square shape slides (5mm  $\times$  5mm), washed with water & ethanol, and then dried before placing into 1 ml selected medium (BHI for VRE and TSB supplemented with 1% glucose for MRSA) placed in a 24 well plate.  $10^6$  CFU/ml bacteria suspension was made by diluting overnight cultured bacteria in PBS buffer. 40  $\mu\text{l}$  of this diluted bacteria suspension was added to each well. The plate was incubated at  $37^\circ\text{C}$  for 24 hours. Catheter samples were removed and washed gently thrice with PBS buffer to remove unattached

bacteria. Stain containing SYTO 9 dye was prepared in filtered sterilized water according to the manufacturer's protocol. The final concentration for SYTO 9 stain was 6  $\mu\text{M}$ . 20  $\mu\text{l}$  of stain solution was added and spread on each catheter slide and incubated in the dark for 15-20 mins before examination under a fluorescence microscope. Fluorescence imaging was done with 488 nm excitation and a 500-550 nm filter in the microscope optical path. In all cases, a 20 $\times$  objective was used, giving a magnification of 400 $\times$ .

### **2.11 Bacterial morphology check under Field Emission Scanning Electron Microscopy**

Catheter samples including control samples (both tube segments and slides) were washed with water & ethanol, and then dried before placing into 1 ml selected medium (BHI for VRE and TSB supplemented with 1% glucose for MRSA) placed in a 24 well plate.  $10^6$  CFU/ml bacteria suspension was made by diluting overnight cultured bacteria in PBS buffer. 40  $\mu\text{l}$  of this diluted bacteria suspension was added to each well. The plate was incubated at 37  $^{\circ}\text{C}$  for 24 hours. Catheter samples were removed and washed gently thrice with PBS buffer to remove unattached bacteria. Each sample was immersed in 2 ml 3% glutaraldehyde in PBS and refrigerated at 4  $^{\circ}\text{C}$  overnight. The samples were dehydrated with a graded concentration series of ethanol/water mixtures (25%, 50%, 75%, 100%). Dehydrated samples were further dried under nitrogen before coating with platinum for FE-SEM.

### **2.12 *In Vivo* mice CAUTI model of catheters**

Briefly, 7 to 8 week old female mice were anesthetized by inhalation of isoflurane and transurethrally implanted with coated and uncoated silicone catheter tubing (5 mm in length). Immediately after implantation, 50  $\mu\text{l}$  of  $1 \times 10^6$  to  $3 \times 10^6$  CFU/ml bacteria in PBS buffer were introduced into the bladder lumen by transurethral inoculation. At the 24 hour time point, animals

were euthanized with CO<sub>2</sub> followed by cervical dislocation. Bladders and kidneys were aseptically harvested. Afterwards, the silicone implants were retrieved from the bladder, placed in PBS buffer, sonicated for 10 min, and then vortexed at maximum speed for 5 mins. The bladder and kidneys from each mouse were homogenized in PBS buffer. Samples were serially diluted and plated on LB agar plates supplemented with appropriate antibiotics. CFU were enumerated after 24 hours of incubation at 37 °C. In all cases, experiments were performed at least twice with n = 5 mice/strain/condition to determine the bacterial load (log reduction).

### **3. Results and discussion**

#### **3.1 Coating synthesis and characterization**

Three coating formulations were investigated (Table 1); each contained uncharged PEGDMA as crosslinker and a cationic monomer of AMPTMA or oligomeric Q-PEI-MA. Q-PEI-MA were chosen for the studies as they are known to have anti-bacterial effects and have different forms of cationic groups: -NH<sub>2</sub> versus -N<sup>+</sup>(R<sub>3</sub>); these oligomers were synthesized in-house and characterized by <sup>1</sup>H NMR (Figure S1 in Supporting information).

X-ray photoelectron spectroscopy (XPS) results (both wide scan and high-resolution N<sub>1s</sub> and C<sub>1s</sub> core-level spectra) of pristine and modified PDMS catheters are shown in Figure 1 and Figure S2. In all samples (pristine, PDA pre-treated (Step 1), BiBB/PDA pre-treated (Step 2) and polymer formulation 1-3 coated PDMS catheters), the XPS wide scans show peaks at 153.2 eV and 102.6 eV corresponding to Si<sub>2s</sub> and Si<sub>2p</sub>, respectively. The C<sub>1s</sub> core-level spectra of all samples (Figure S2) show peaks at 284.6 eV and 286.7 eV corresponding respectively to C-C/C-H and C-O in PDMS. For the PDA/PDMS sample (Step 1), the N<sub>1s</sub> core level spectra (Figure 1 (C), b), as well as the wide XPS scan (Figure 1(A), b), shows a new peak at 400.0 eV attributed to PDA,

specifically to its predominant secondary amine groups of indole, non-protonated and protonated primary amine, and imine functionalities;<sup>30</sup> the C<sub>1s</sub> core-level spectra of the PDA coating (Figure S2 B) shows two new peaks at 285.6 eV and 288.6 eV corresponding to C-N and -C=O. The FTIR-ATR spectra of PDA/PDMS sample (Step 1) show new peaks at 3200-3300 cm<sup>-1</sup> corresponding to -OH/-NH<sub>2</sub> groups because of the PDA coating (Figure S4 (A)). For Sample c (Step 2) with normal BiBB initiator anchored on the PDMS catheter, the XPS wide scan (Figure 1(A), c) and core-level spectra (Figure 1 (B)) show two new peaks at 67.5 and 68.5 eV which correspond to Br<sub>3d</sub>, corroborating the successful grafting of the initiator.<sup>27</sup> In the FTIR-ATR spectra of the BiBB-anchored sample (Figure S4 (A) Step 2), a new peak appeared at 1644 cm<sup>-1</sup>, attributable to the stretching of the ester carbonyl group from the BiBB initiator.<sup>31</sup> The N<sub>1s</sub> core level spectra of the same sample c (Figure 1 (C), c) shows a new peak at 401.9 eV corresponding to O=C-N which is attributed to BiBB. In the N<sub>1s</sub> core level spectra of coating 1 (Figure 1 (C), d), the peak areas of -N<sup>+</sup>-H group at 402.2 eV and -N-H group at 400.0 eV are the same and are attributed respectively to equimolar quaternary amine group and amide groups on the side chain of AMPTMA.

For the N<sub>1s</sub> core level spectra of coating 2 (Figure 1 (C), e), the peak area of -N<sup>+</sup>-H peak is stronger than that of -N-H group, which corroborates the presence of a high concentration of quaternized amine groups and imine groups from the Q-PEI-MA. This is reinforced by the fact that for coating 2 (Table 1 and Table 2), the [N]/[Si] ratio is 0.75:1 and [C-N]/[C-C/C-H] is 0.578 in the C<sub>1s</sub> core level spectra, both of which are higher than in the other coatings. Coatings 3 (Figure 1 (C), f) has smaller peak areas in N<sub>1s</sub> core level spectra than coating 1, and coating 2, due to the absence of AMPTMA in their formulations.

We also characterized the surfaces of Low Density BiBB (Step 2 (LD)), normal density (Step 2) and High Density BiBB (Step 2 (HD)) coated surfaces. From the XPS spectrum (Figure S3 (A)),

there is difference in the intensities of the  $\text{Br}_{3d}$  peak (68 eV) from the Step 2 (LD) surface initiator versus that of Step 2 (HD); the  $[\text{Br}]/[\text{Si}]$  for Step 2 (normal density), Step 2 (LD) and Step 2 (HD) are 0.83, 0.58 and 0.94 (Table 2) respectively, corroborating that higher densities of surface BiBB initiator result in higher XPS signal. The FTIR-ATR spectra (Figure S4 (A)) show that the surface after Step 2 (HD) has higher ester carbonyl group ( $1644\text{ cm}^{-1}$ ) intensity than coating after Step 2 (LD) and Step 2 (normal), corroborating that BiBB with different initiator densities have been prepared. We also did the XPS and FTIR-ATR analysis of coating 1 with different BiBB densities. The  $\text{N}_{1s}$  core-level spectra of coating 1 (LD) (Figure S3 (F), bottom) shows a smaller peak area of  $-\text{N}^+-\text{H}$  at 402.2 eV compared to the  $-\text{N}-\text{H}$  peak at 400.0 eV, in contrast to those of coating 1 (HD, top), indicating that low grafting density BiBB leads to thinner AMPTMA/PEGDMA coating. With FTIR-ATR, the intensities of  $-\text{NH}$  group at  $1510\text{ cm}^{-1}$  (Figure S4 (B)) for the coating 1 (LD) and coating 1 (normal) corroborates with the BiBB coating density; for the coating 1 (HD), the intensities of  $-\text{NH}$  group peak is the almost same as coating 1 since the latter is almost quite fully covered by coating 1.

Figure 2 shows FE-SEM images of the inside surfaces of pristine PDMS catheter and coatings 1, 2 and 3. All the coatings cover the PDMS catheter inner surface uniformly. All coatings are clearly visible in cross-section images of coated catheters in Figure S7. Coating 1 is a few microns thick showed in Figure S7 (B) and its contact angle decreased from  $109.3^\circ$  (for PDMS) to  $32.7^\circ$  (Table 2 and Figure S5) due to the hydrophilic amide groups in poly(AMPTMA) chains that are cross-linked with PEGDMA. The coating 1 (LD) inner surface (Figure S6 (A)) exhibits non-uniform and coating thickness (less than  $2\text{ }\mu\text{m}$ ) compared with coating 1 (Figure 2 (B) and Figure S7 (B)), and the contact angle is also increased to  $64.9^\circ$  (Table 2); coating 1 (HD) (Figure S6 (D)) exhibits thicker coating (about  $10\text{ }\mu\text{m}$ ) and the contact angle was decreased to  $23.3^\circ$  (Table 2) indicating a

hydrophilic surface. Inclusion of poly(Q-PEI-MA) (coating 2) into the APMPTA/PEGDMA formulation 1 increases the thickness of the corresponding coatings 2 (Figure S7 (C)), and also increases its contact angles to 49.1°. The higher contact angles can be attributed to the fact that, compared to poly(AMPTMA), coating 2 containing poly(Q-PEI-MA), has more hydrophobic quaternized amine groups. On the other hand, coatings 3 (Figure S7 (D)) are thinner (about 7 µm) and have high contact angles (96.6°); this is due to the absence of hydrophilic poly(AMPTMA) chains, which is also indicated by the decreased 402.2 eV peaks in the N<sub>1s</sub> core level spectra (Figure 1 (C), f).

Changes in the surface morphology of the coatings were characterized by AFM. Clear differences in unmodified PDMS, PDA coated PDMS and different coatings of PDMS catheters are evident in Figure S8 and Figure S9. The pristine PDMS catheter shown in Figure S8 (A) presents a relatively smooth, compact and microscopically homogeneous surface, with an average roughness (R<sub>a</sub>) of 14.2 nm. After coating PDA on the catheter surface, the R<sub>a</sub> of modified surface increased to 24.7 nm. (The thickness of PDA coating on the catheter is about 20 nm from AFM (Figure S8 (B)), specifically, we measured the depth of the step PDA coating created by immersing only half of PDMS catheter into the PDA coating solution.) The R<sub>a</sub> of coatings 1-3 are 66.9 nm, 119 nm, 72.0 nm (Figure S9), respectively, consistently 1-2% of the coating thickness. These roughness measures correspond to the vertical scale of the nodular structures observed with FE-SEM examination (Figure S7). Furthermore, the R<sub>a</sub> of coating 1 (LD) and coating 1 (HD) are 56.4 nm and 164.0 nm, respectively, compared to 66.9 nm for the control (medium) density coating 1, indicating that the roughness correlates to the grafting density (Figure S8 (C), (D)).

### **3.2 Anti-biofilm/anti-bacterial assay *in Vitro***

Figure 3 (A) shows the *in vitro* anti-bacterial/anti-biofilm activities of coated PDMS catheters compared with unmodified PDMS catheter. The PDMS catheter permits colonization by MRSA and VRE bacteria; using our protocols, the bacterial cell counts are in the range of  $1 \times 10^6$  -  $3 \times 10^6$  CFU/ml respectively. The coating 1 can produce more than 2.00 log (99.00%) reduction when challenged with MRSA *in vitro*, while additional Q-PEI-MA components in the film coating 2 make the log reductions worse. When challenged with VRE, film coating 1 showed less than 0.50 log (68.38%) reduction. However, larger than 1 log (90.00%) reduction was achieved by coatings 2, with coating 2 reaching 1.50 log (96.84%) reduction. Coating 3, which contained just Q-PEI-MA and PEGDMA, showed balanced anti-biofilm/anti-bacterial activity for MRSA and VRE, with 1.60 log (97.49%) reduction and 1.10 log (92.06%) reduction, respectively.

With lower BiBB initiator, the coating 1 (LD) only achieves 1.10 log (92.06%) reduction of MRSA (Table S2), compared to 2.10 log (99.21%) reduction for coating 1 (Figure 3 (A)). Interestingly, with higher BiBB surface grafting density (coating 1 HD), the coating also becomes much more hydrophilic but achieves similar antibiofilm killing effect of 1.77 log (98.30%) reduction for MRSA compared with coating 1.

From Figure 3 (A), without autoclave, coating 1 and coating 2 achieved 2.10 log (99.21%) reduction and 1.50 log (96.84%) for MRSA and VRE, respectively. We also studied the effect of autoclave on these bactericidal activity; coating 1 after autoclave (denoted by AC) still maintained 1.85 log (98.59%) reduction for MRSA while coating 2 (AC) reached 1.36 log (95.63%) reduction for VRE, respectively (see Table S2), indicating that the anti-biofilm activity of our coatings was not affected by high temperature and pressure treatment.

We also investigated longer (5 cm rather than 5 mm) catheters with three diameters (0.3 mm which is the standard diameter used in this paper generally needed for animal test, 1 mm and 8 mm inner diameters) (Figure S10). Generally, the ends (the last 1.0 cm or so sections) can reach the same log reduction (about 1.80 log (98.42%) reduction) but as we progress inwards, the bacteria killing efficacy decreases to about 1.00 log (90%) reduction. For coating of long catheters, we propose that the reaction fluid shall be pumped through the outer and inner surfaces of the catheters with a specially-designed reactor.

### **3.3 Hemolytic activity of modified PDMS catheter**

Figure 3 (B) shows the degree of hemolysis produced by unmodified and coated PDMS catheters. The degree of hemolysis of unmodified PDMS catheter was ~0.3%. PDMS catheters with coatings 1, 2 showed slightly higher hemolysis degrees than unmodified PDMS catheter, with film coating 2 having the least favorable hemolysis, 1.3%, due to its high concentration of charge in poly(Q-PEI-MA). According to the American Society for Testing and Materials (ASTM) F756-00 standard,<sup>32</sup> a hemolysis degree of 2% or less is considered non-hemolytic for biomaterials; by this standard all anti-bacterial film coatings reported here are hemocompatible. Coatings 3 exhibit hemolysis similar to that of unmodified PDMS catheter due to their high contact angle and low surface charge.

### **3.4 Cytocompatibility Assay *in Vitro***

To evaluate the potential cytotoxicity of coated PDMS catheters, the cell viability of 3T3 fibroblast cells with coated catheter samples immersed in the culture medium was measured by MTT (3-(4, 5-dimethylthiazolyl-2)-2, 5-diphenyl tetrazolium bromide) testing. After 24-hour incubation with samples, the 3T3 cell viability was above 95% (Figure 3 (C)) in all cases and was

not significantly different from that of control sample. The PDMS catheter in our experiment has been approved by the U.S. Food and Drug Administration (FDA) and is widely used clinically and our coating is designed to be non-leaching and biocompatible, so this result is unsurprising.

### **3.5 Anti-bacterial assay *in Vivo***

Coatings 1 and 2, which respectively showed the best *in vitro* anti-bacterial activities against MRSA and VRE, were tested *in vivo*. As shown in Figure 4, the *in vivo* log reductions of bacteria on the surface of the catheter with coating 1 for MRSA and coating 2 for VRE were 1.95 log (98.88%) reduction and 1.26 log (94.51%) reduction, respectively, which were only slightly less than those for the *in vitro* assays, indicating that the two formulations retain their anti-bacterial performance in the more complex *in vivo* environment. ~~Bacteria grown in the bladder & kidney were also quantified (Figure S11 and S12). Despite the significant reduction in colonization on coated catheters, infection in these two organs was not prevented, because the anti-biofilm coatings onto the catheters are non-leachable.~~

### **3.6 Mechanistic study**

The mechanism of anti-bacterial activity of the polycationic film coated PDMS catheters against MRSA and VRE was examined by fluorescence microscopy and FE-SEM. Fluorescence microscopy and FE-SEM images showed large numbers of MRSA on unmodified PDMS catheter and the green fluorescence in Figure 5 shows that the MRSA cells are alive. The dense clusters of bacteria (Figure 5 (A)) indicate that PDMS permits biofilm formation, which is attributable to its hydrophobic character.<sup>33</sup> On coating 1 surface, both FE-SEM and fluorescence microscopy show the number of viable MRSA cells to be greatly reduced, confirming the anti-MRSA nature of the AMPTMA-PEGDMA film coating 1 (Figure 5 (B)). With bacterial cell membranes, coating 1 is

much more hydrophilic making it more anti-fouling to reduce the interactions.<sup>1,34</sup> Coatings 2 and 3 both also have reduced MRSA on their surfaces (Figure 5 (C) and (D)). Interestingly, although coating 3 has larger contact angle and smooth surface morphology, it also prohibits formation of MRSA biofilm, probably because of the large amount of surface cationic charges due to the poly(Q-PEI-MA) constituent. We also examined the colonization of the catheter surfaces by VRE using FE-SEM and fluorescence microscopy. Coating 2 formulated with AMPTMA, PEGDMA and Q-PEI-MA achieved significant reduction of viable VRE compared with unmodified PDMS (Figure 6 (A, a) and (B, b)). It appears that poly(Q-PEI-MA) is effective in inhibiting VRE, but poly(AMPTMA) cannot. Poly(AMPTMA) (coating 1) causes increased hydrophilicity and reduces fouling by MRSA bacteria. Poly(Q-PEI-MA) (coating 3) has polar permanent ammonium charges and is effective against MRSA and VRE.

### **3.7 Discussion**

Inserted catheter-associated infection is a common form of nosocomial infection. One reason for this phenomenon could be attributed to the increasing insertion of prosthetic medical devices such as catheter, as any foreign body which provides a site for biofilm growth.<sup>35</sup> Any inserted or implanted foreign body provides a substrate for biofilm growth and catheter-associated infections are common on account of the widespread use of catheters and the difficulty of perfectly sterile placement. These infections come about when planktonic microorganisms adhere to the catheter surface and produce extracellular polymers that enable more microorganisms to adhere onto the surface, forming a biofilm.<sup>36</sup> As established biofilms are resistant to both host defences and conventional antimicrobial therapy, it is highly desirable to modify catheters to be both anti-bacterial and anti-biofilm.<sup>37-38</sup>

Our coating comprises the right balance of cationic charge and hydrophilic PEG to make the coating anti-bacterial and anti-biofilm. The suitable *in vitro* biofilm testing quite closely mimics the *in vivo* biofilm mouse model. The addition of PEGDMA adds hydrophilicity to the coating to minimise the Tryptic Soy Broth (TSB) protein adsorption but when bacteria do get eventually attracted to the surface, the concentrated cationic charges do kill bacterial by contact. Coating 1 (flat film) is the most hydrophilic with the lowest contact angle of 34.1° (Table S3) and it also has fairly high cationic charge density as measured by the surface zeta potential (17.1±0.5, Table S3). Coating 2 and 3 are more hydrophobic and hence result in poorer antibiofilm effect.

“Grafting from” a catheter surface offers a route for covalent bonding of the polymer to the catheter. Amongst various “grafting from” techniques, surface-initiated atom transfer radical polymerization (SI-ATRP) offers versatility in the range of monomers that can be employed.<sup>39-41</sup> We have demonstrated a unique method of coating a film onto PDMS catheter based in SI-ATRP that avoids UV and argon plasma treatment, which are not easy to implement for long slender tubular-shaped catheters. The SI-ATRP grafting method also ensures strong covalent linkage of the coating to the catheter and is also suitable for aqueous phase polymerization. Jiang *et al.* reported a coating of a super-hydrophilic material onto polydimethylsiloxane (PDMS) using zwitterionic poly(carboxybetaine methacrylate) (pCBMA) brush *via* SI-ATRP. The prepared PDMS functional coating exhibited reduced nonspecific protein adsorption in complex media.<sup>42</sup> Recently, supplemental activator and reducing agent surface-initiated atom transfer radical polymerization (SARA ATRP) was developed,<sup>43-46</sup> which uses Cu<sup>I</sup> and Cu<sup>II</sup> as activators and deactivators, respectively. When Cu<sup>0</sup> is used in the reaction, it slowly generates the radical species and Cu<sup>I</sup>X as a reducing agent *via* supplemental activation.<sup>47-50</sup> SARA ATRP stabilizes the *in situ*

Cu<sup>I</sup> species at low oxygen levels so that it may be successfully performed in aqueous mixture solvent to prepare well-defined biopolymers.<sup>46, 51</sup>

A limitation of many studies relating to antifouling or anti-bacterial effect of coated hydrophilic polymers is that they have used model flat films rather than tubular catheters.<sup>52-54</sup> Catheters used for human medical applications have relatively small diameters; for example, Foley catheters typically vary in size from 1 mm to about 10 mm. Plasma and UV pre-treatment processes for achieving uniform hydrophilization of both the inner and outer surfaces are typically difficult over the length of small diameter plastic catheter. Unlike model flat surfaces, coatings on tubular catheters tend not to be uniform with UV or plasma pre-treatment.<sup>55</sup>

Various polydopamine-assisted antibacterial and antibiofilm coatings have been developed,<sup>56</sup> but some involve the diffusion of leachable antibacterial components such as silver;<sup>38</sup> so that the PEG makes the surface antifouling while the silver release causes the bacteria to be killed. Other reports involve enzymes which are usually specific to certain bacteria and expensive;<sup>57</sup> for example, lysostaphin is a highly specific anti-staphylococcal endopeptidase.<sup>58</sup> Also, we show that our coated catheter can have *in vivo* antibiofilm effect, and not just with *in vitro* testing.

Most commercial catheters are made from PDMS, which is non-toxic, economical, has good thermal and oxidative stability and outstanding mechanical properties.<sup>59-61</sup> However, the extremely hydrophobic nature of PDMS could cause adverse reactions such as ulceration, tissue irritation, significant protein and cell adhesion resulting in biofouling, therefore limiting applications of PDMS catheters.<sup>62-64</sup> Our coating also makes the PDMS hydrophilic and lubricous.

#### **4. Conclusions**

Three anti-bacterial and anti-biofilm non-leachable coatings on PDMS catheter were prepared successfully by SARA SI-ATRP, as confirmed by XPS, AFM and FE-SEM characterizations. This is one of few reports of *in vivo* anti-biofilm coatings with strong linkage to the catheter and are non-leachable against various MDR bacteria. AMPTMA/ PEGDMA film coating exhibits good anti-biofilm and antimicrobial effect against MRSA by having high hydrophilicity with high charge density, with 2.21 log (99.38%) reduction achieved with *in vitro* and 1.95 log (98.88%) reduction with *in vivo* tests. AMPTMA/PEGDMA/Q-PEI-MA film coating has significant efficacy against VRE, with 1.50 log (96.84%) reduction achieved *in vitro* and 1.26 log (94.51%) reduction *in vivo*. All the coatings on the PDMS catheters exhibited low hemolysis and high cell viability, and could be used as biomedical materials. This approach to the formation of uniform non-hemolytic and biocompatible anti-bacterial and anti-biofilm surfaces may also be useful for other kinds of medical devices, particularly those with complex or inaccessible surfaces which may be difficult to uniformly surface treat using approaches such as plasma treatment or UV-initiated polymerization.

## ASSOCIATED CONTENT

### Supporting Information

The Supporting Information is available free of charge on the ACS Publications website at DOI: zeta potential and MIC measurements of monomer; <sup>1</sup>H NMR of polymer; XPS C<sub>1s</sub> core level spectra, contact angle of surface coatings, FE-SEM and AFM of surfaces coatings; and CFU count *in vivo* of bladder and kidney.

## AUTHOR INFORMATION

### Corresponding Author

\* [mbechan@ntu.edu.sg](mailto:mbechan@ntu.edu.sg)

## ORCID

ET Kang: 0000-0003-0599-7834

Hongwei Duan: 0000-0003-2841-3344

Mary B. Chan-Park: 0000-0003-3761-7517

## Notes

The authors declare no competing financial interest.

## ACKNOWLEDGMENT

We thank the funding support from a Singapore Ministry of Education Tier 3 grant (MOE2013-T3-1-002) and a Singapore Ministry of Health Industry Alignment Fund (NMRC/MOHIAFCAT2/003/2014). Wu appreciates NTU for a PhD scholarship. We also thank Celestine Loh Jia Ling for her assistance.

## REFERENCES

- (1) von Eiff, C.; Jansen, B.; Kohnen, W.; Becker, K. Infections Associated with Medical Devices - Pathogenesis, Management and Prophylaxis. *Drugs* **2005**, *65*, 179-214.
- (2) Darouiche , R. O.; Raad , I. I.; Heard , S. O.; Thornby , J. I.; Wenker , O. C.; Gabrielli , A.; Berg , J.; Khardori , N.; Hanna , H.; Hachem , R.; Harris , R. L.; Mayhall , G. A Comparison of Two Antimicrobial-Impregnated Central Venous Catheters. *N. Engl. J. Med.* **1999**, *340*, 1-8.
- (3) Colletta, A.; Wu, J. F.; Wo, Y. Q.; Kappler, M.; Chen, H.; Xi, C. W.; Meyerhoff, M. E. S-Nitroso-N-Acetylpenicillamine (Snap) Impregnated Silicone Foley Catheters: A Potential

- Biomaterial/Device to Prevent Catheter-Associated Urinary Tract Infections. *ACS Biomater. Sci. Eng.* **2015**, *1*, 416-424.
- (4) Warren, J. W. Catheter-Associated Urinary Tract Infections. *Int. J. Antimicrob. Agents* **2001**, *17*, 299-303.
- (5) Smith, A. W. Biofilms and Antibiotic Therapy: Is There a Role for Combating Bacterial Resistance by the Use of Novel Drug Delivery Systems? *Adv. Drug Del. Rev.* **2005**, *57*, 1539-1550.
- (6) Lam, T. B. L.; Omar, M. I.; Fisher, E.; Gillies, K.; MacLennan, S. Types of Indwelling Urethral Catheters for Short-Term Catheterisation in Hospitalised Adults. *Cochrane Database of Systematic Reviews* **2014**, 1-92.
- (7) Hachem, R.; Reitzel, R.; Borne, A.; Jiang, Y.; Tinkey, P.; Uthamanthil, R.; Chandra, J.; Ghannoum, M.; Raad, I. Novel Antiseptic Urinary Catheters for Prevention of Urinary Tract Infections: Correlation of in Vivo and in Vitro Test Results. *Antimicrob. Agents Chemother.* **2009**, *53*, 5145-5149.
- (8) Tenke, P.; Koves, B.; Johansen, T. E. B. An Update on Prevention and Treatment of Catheter-Associated Urinary Tract Infections. *Curr. Opin. Infect. Dis.* **2014**, *27*, 102-107.
- (9) Pickard, R.; Lam, T.; MacLennan, G.; Starr, K.; Kilonzo, M.; McPherson, G.; Gillies, K.; McDonald, A.; Walton, K.; Buckley, B.; Glazener, C.; Boachie, C.; Burr, J.; Norrie, J.; Vale, L.; Grant, A.; N'Dow, J. Antimicrobial Catheters for Reduction of Symptomatic Urinary Tract Infection in Adults Requiring Short-Term Catheterisation in Hospital: A Multicentre Randomised Controlled Trial. *The Lancet* **2012**, *380*, 1927-1935.
- (10) Pai, M. P.; Pendland, S. L.; Danziger, L. H. Antimicrobial-Coated/Bonded and -Impregnated Intravascular Catheters. *Ann. Pharmacother.* **2001**, *35*, 1255-1263.

- (11) Wang, W.; Lu, Y.; Xie, J.; Zhu, H.; Cao, Z. A Zwitterionic Macro-Crosslinker for Durable Non-Fouling Coatings. *Chem. Commun.* **2016**, *52*, 4671-4674.
- (12) Waschinski, C. J.; Zimmermann, J.; Salz, U.; Hutzler, R.; Sadowski, G.; Tiller, J. C. Design of Contact - Active Antimicrobial Acrylate - Based Materials Using Biocidal Macromers. *Adv. Mater.* **2008**, *20*, 104-108.
- (13) Furno, F.; Morley, K. S.; Wong, B.; Sharp, B. L.; Arnold, P. L.; Howdle, S. M.; Bayston, R.; Brown, P. D.; Winship, P. D.; Reid, H. J. Silver Nanoparticles and Polymeric Medical Devices: A New Approach to Prevention of Infection? *J. Antimicrob. Chemother.* **2004**, *54*, 1019-1024.
- (14) Noimark, S.; Dunnill, C. W.; Wilson, M.; Parkin, I. P. The Role of Surfaces in Catheter-Associated Infections. *Chem. Soc. Rev.* **2009**, *38*, 3435-3448.
- (15) Dave, R. N.; Joshi, H. M.; Venugopalan, V. P. Novel Biocatalytic Polymer-Based Antimicrobial Coatings as Potential Ureteral Biomaterial: Preparation and in Vitro Performance Evaluation. *Antimicrob. Agents Chemother.* **2011**, *55*, 845-853.
- (16) Wong, I.; Ho, C. M. Surface Molecular Property Modifications for Poly(Dimethylsiloxane) (Pdms) Based Microfluidic Devices. *Microfluid. Nanofluid.* **2009**, *7*, 291-306.
- (17) Tu, Q.; Wang, J.-C.; Liu, R.; He, J.; Zhang, Y.; Shen, S.; Xu, J.; Liu, J.; Yuan, M.-S.; Wang, J. Antifouling Properties of Poly(Dimethylsiloxane) Surfaces Modified with Quaternized Poly(Dimethylaminoethyl Methacrylate). *Colloids Surf. B. Biointerfaces* **2013**, *102*, 361-370.
- (18) Monteiro, D.; Gorup, L.; Silva, S.; Negri, M.; de Camargo, E.; Oliveira, R.; Barbosa, D. d. B.; Henriques, M. Silver Colloidal Nanoparticles: Antifungal Effect against Adhered Cells and Biofilms of *Candida Albicans* and *Candida Glabrata*. *Biofouling* **2011**, *27*, 711-719.

- (19) Li, M.; Neoh, K. G.; Xu, L. Q.; Wang, R.; Kang, E.-T.; Lau, T.; Olszyna, D. P.; Chiong, E. Surface Modification of Silicone for Biomedical Applications Requiring Long-Term Antibacterial, Antifouling, and Hemocompatible Properties. *Langmuir* **2012**, *28*, 16408-16422.
- (20) Hellmich, W.; Regtmeier, J.; Duong, T. T.; Ros, R.; Anselmetti, D.; Ros, A. Poly (Oxyethylene) Based Surface Coatings for Poly (Dimethylsiloxane) Microchannels. *Langmuir* **2005**, *21*, 7551-7557.
- (21) Wang, Y.; Lai, H.-H.; Bachman, M.; Sims, C. E.; Li, G.; Allbritton, N. L. Covalent Micropatterning of Poly (Dimethylsiloxane) by Photografting through a Mask. *Anal. Chem.* **2005**, *77*, 7539-7546.
- (22) Hu, S.; Ren, X.; Bachman, M.; Sims, C. E.; Li, G.; Allbritton, N. Surface Modification of Poly (Dimethylsiloxane) Microfluidic Devices by Ultraviolet Polymer Grafting. *Anal. Chem.* **2002**, *74*, 4117-4123.
- (23) Shi, Q.; Ye, S.; Spanninga, S. A.; Su, Y.; Jiang, Z.; Chen, Z. The Molecular Surface Conformation of Surface-Tethered Polyelectrolytes on Pdms Surfaces. *Soft Matter* **2009**, *5*, 3487-3494.
- (24) Mokkaphan, J.; Banlunara, W.; Palaga, T.; Sombuntham, P.; Wanichwecharungruang, S. Silicone Surface with Drug Nanodepots for Medical Devices. *ACS Appl. Mater. Interfaces* **2014**, *6*, 20188-20196.
- (25) Pascual, A. Pathogenesis of Catheter - Related Infections: Lessons for New Designs. *Clin. Microbiol. Infect.* **2002**, *8*, 256-264.
- (26) Tenke, P.; Riedl, C. R.; Jones, G. L.; Williams, G. J.; Stickler, D.; Nagy, E. Bacterial Biofilm Formation on Urologic Devices and Heparin Coating as Preventive Strategy. *Int. J. Antimicrob. Agents* **2004**, *23*, 67-74.

- (27) Yu, B.-Y.; Zheng, J.; Chang, Y.; Sin, M.-C.; Chang, C.-H.; Higuchi, A.; Sun, Y.-M. Surface Zwitterionization of Titanium for a General Bio-Inert Control of Plasma Proteins, Blood Cells, Tissue Cells, and Bacteria. *Langmuir* **2014**, *30*, 7502-7512.
- (28) Le-Masurier, S. P.; Duong, H. T. T.; Boyer, C.; Granville, A. M. Surface Modification of Polydopamine Coated Particles Via Glycopolymer Brush Synthesis for Protein Binding and Flim Testing. *Polym. Chem.* **2015**, *6*, 2504-2511.
- (29) Guiton, P. S.; Hung, C. S.; Hancock, L. E.; Caparon, M. G.; Hultgren, S. J. Enterococcal Biofilm Formation and Virulence in an Optimized Murine Model of Foreign Body-Associated Urinary Tract Infections. *Infect. Immun.* **2010**, *78*, 4166-4175.
- (30) Surman, F.; Riedel, T.; Bruns, M.; Kostina, N. Y.; Sedláková, Z.; Rodriguez - Emmenegger, C. Polymer Brushes Interfacing Blood as a Route toward High Performance Blood Contacting Devices. *Macromol. Biosci.* **2015**, *15*, 636-646.
- (31) Fristrup, C. J.; Jankova, K.; Hvilsted, S. Hydrophilization of Poly (Ether Ether Ketone) Films by Surface-Initiated Atom Transfer Radical Polymerization. *Polym. Chem.* **2010**, *1*, 1696-1701.
- (32) Bauer, M.; Lautenschlaeger, C.; Kempe, K.; Tauhardt, L.; Schubert, U. S.; Fischer, D. Poly (2 - Ethyl - 2 - Oxazoline) as Alternative for the Stealth Polymer Poly (Ethylene Glycol): Comparison of in Vitro Cytotoxicity and Hemocompatibility. *Macromol. Biosci.* **2012**, *12*, 986-998.
- (33) Kane, R. S.; Deschatelets, P.; Whitesides, G. M. Kosmotropes Form the Basis of Protein-Resistant Surfaces. *Langmuir* **2003**, *19*, 2388-2391.
- (34) Hoque, J.; Akkapeddi, P.; Yadav, V.; Manjunath, G. B.; Uppu, D. S.; Konai, M. M.; Yarlagadda, V.; Sanyal, K.; Haldar, J. Broad Spectrum Antibacterial and Antifungal Polymeric

Paint Materials: Synthesis, Structure–Activity Relationship, and Membrane-Active Mode of Action. *ACS Appl. Mater. Interfaces* **2015**, *7*, 1804-1815.

(35) Guggenbichler, J. P.; Assadian, O.; Boeswald, M.; Kramer, A. Incidence and Clinical Implication of Nosocomial Infections Associated with Implantable Biomaterials-Catheters, Ventilator-Associated Pneumonia, Urinary Tract Infections. *GMS Krankenhaushygiene interdisziplinär* **2011**, *6*, 1-19.

(36) Donlan, R. M. Biofilms and Device-Associated Infections. *Emerg. Infect. Dis.* **2001**, *7*, 277-81.

(37) Lim, K.; Chua, R. R. Y.; Ho, B.; Tambyah, P. A.; Hadinoto, K.; Leong, S. S. J. Development of a Catheter Functionalized by a Polydopamine Peptide Coating with Antimicrobial and Antibiofilm Properties. *Acta Biomater.* **2015**, *15*, 127-138.

(38) Sileika, T. S.; Kim, H.-D.; Maniak, P.; Messersmith, P. B. Antibacterial Performance of Polydopamine-Modified Polymer Surfaces Containing Passive and Active Components. *ACS Appl. Mater. Interfaces* **2011**, *3*, 4602-4610.

(39) Wei, Q.; Wang, X.; Zhou, F. A Versatile Macro-Initiator with Dual Functional Anchoring Groups for Surface-Initiated Atom Transfer Radical Polymerization on Various Substrates. *Polym. Chem.* **2012**, *3*, 2129-2137.

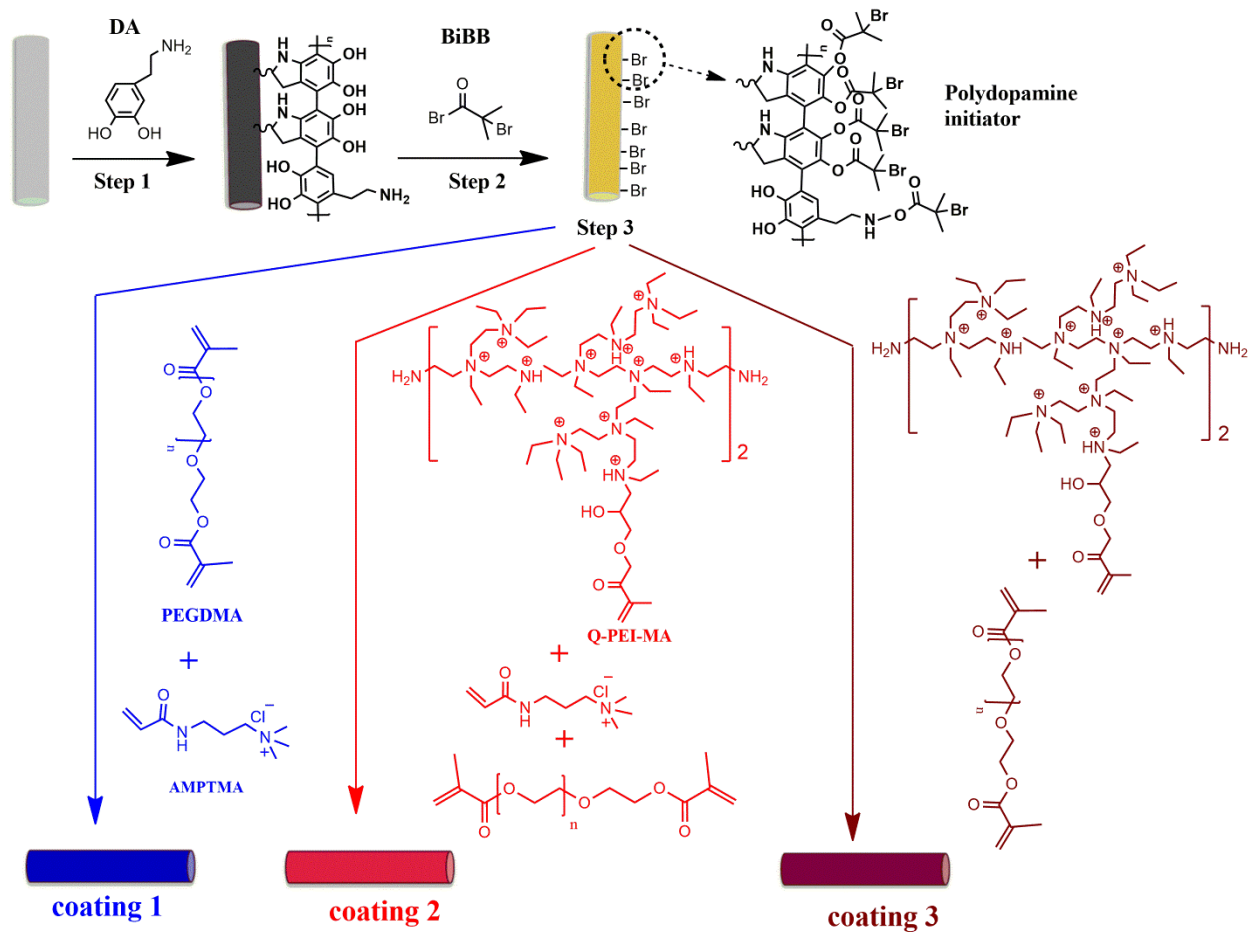
(40) Chaudhary, O. J.; Calius, E. P.; Kennedy, J. V.; Dickinson, M.; Loho, T.; Travas-Sejdic, J. Bioinspired Dry Adhesive: Poly (Dimethylsiloxane) Grafted with Poly (2-Ethylhexyl Acrylate) Brushes. *Eur. Polym. J.* **2015**, *68*, 432-440.

(41) Chen, T.; Jordan, R.; Zauscher, S. Extending Micro-Contact Printing for Patterning Complex Polymer Brush Microstructures. *Polymer* **2011**, *52*, 2461-2467.

- (42) Keefe, A. J.; Brault, N. D.; Jiang, S. Suppressing Surface Reconstruction of Superhydrophobic Pdms Using a Superhydrophilic Zwitterionic Polymer. *Biomacromolecules* **2012**, *13*, 1683-1687.
- (43) Konkolewicz, D.; Wang, Y.; Zhong, M.; Krys, P.; Isse, A. A.; Gennaro, A.; Matyjaszewski, K. Reversible-Deactivation Radical Polymerization in the Presence of Metallic Copper. A Critical Assessment of the Sara Atrp and Set-Lrp Mechanisms. *Macromolecules* **2013**, *46*, 8749-8772.
- (44) Konkolewicz, D.; Wang, Y.; Krys, P.; Zhong, M.; Isse, A. A.; Gennaro, A.; Matyjaszewski, K. Sara Atrp or Set-Lrp. End of Controversy? *Polym. Chem.* **2014**, *5*, 4396-4417.
- (45) Abreu, C. M.; Serra, A. C.; Popov, A. V.; Matyjaszewski, K.; Guliashvili, T.; Coelho, J. F. Ambient Temperature Rapid Sara Atrp of Acrylates and Methacrylates in Alcohol–Water Solutions Mediated by a Mixed Sulfite/Cu (I) Br<sub>2</sub> Catalytic System. *Polym. Chem.* **2013**, *4*, 5629-5636.
- (46) Konkolewicz, D.; Krys, P.; Góis, J. R.; Mendonça, P. V.; Zhong, M.; Wang, Y.; Gennaro, A.; Isse, A. A.; Fantin, M.; Matyjaszewski, K. Aqueous Rdrp in the Presence of Cu<sub>0</sub>: The Exceptional Activity of Cu<sub>I</sub> Confirms the Sara Atrp Mechanism. *Macromolecules* **2014**, *47*, 560-570.
- (47) Cordeiro, R. A.; Rocha, N.; Mendes, J. P.; Matyjaszewski, K.; Guliashvili, T.; Serra, A. C.; Coelho, J. F. Synthesis of Well-Defined Poly (2-(Dimethylamino) Ethyl Methacrylate) under Mild Conditions and Its Co-Polymers with Cholesterol and Peg Using Fe (0)/Cu (I) Based Sara Atrp. *Polym. Chem.* **2013**, *4*, 3088-3097.
- (48) Mendonça, P. V.; Konkolewicz, D.; Averick, S. E.; Serra, A. C.; Popov, A. V.; Guliashvili, T.; Matyjaszewski, K.; Coelho, J. F. Synthesis of Cationic Poly ((3-Acrylamidopropyl) Trimethylammonium Chloride) by Sara Atrp in Ecofriendly Solvent Mixtures. *Polym. Chem.* **2014**, *5*, 5829-5836.

- (49) Zhang, Y.; Wang, Y.; Matyjaszewski, K. Atrp of Methyl Acrylate with Metallic Zinc, Magnesium, and Iron as Reducing Agents and Supplemental Activators. *Macromolecules* **2011**, *44*, 683-685.
- (50) Kryszewski, P.; Wang, Y.; Matyjaszewski, K.; Harrison, S. Radical Generation and Termination in ATRP of Methyl Acrylate: Effect of Solvent, Ligand, and Chain Length. *Macromolecules* **2016**, *49*, 2977-2984.
- (51) Abreu, C. M.; Mendonça, P. V.; Serra, A. n. C.; Popov, A. V.; Matyjaszewski, K.; Guliashvili, T.; Coelho, J. F. Inorganic Sulfites: Efficient Reducing Agents and Supplemental Activators for Atom Transfer Radical Polymerization. *ACS Macro Lett.* **2012**, *1*, 1308-1311.
- (52) Huang, C.-F. Surface-Initiated Atom Transfer Radical Polymerization for Applications in Sensors, Non-Biofouling Surfaces and Adsorbents. *Polym. J.* **2016**, *48*, 341-350.
- (53) Li, B.; Yu, B.; Ye, Q.; Zhou, F. Tapping the Potential of Polymer Brushes through Synthesis. *Acc. Chem. Res.* **2014**, *48*, 229-237.
- (54) Krishnamoorthy, M.; Hakobyan, S.; Ramstedt, M.; Gautrot, J. E. Surface-Initiated Polymer Brushes in the Biomedical Field: Applications in Membrane Science, Biosensing, Cell Culture, Regenerative Medicine and Antibacterial Coatings. *Chem. Rev.* **2014**, *114*, 10976-11026.
- (55) Zhou, C.; Zhang, H. W.; Jiang, Y.; Wang, W. J.; Yu, Q. Grafting of Polyacrylamide from Poly (Ethylene Terephthalate) Films. *J. Appl. Polym. Sci.* **2011**, *121*, 1254-1261.
- (56) Lee, H.; Dellatore, S. M.; Miller, W. M.; Messersmith, P. B. Mussel-Inspired Surface Chemistry for Multifunctional Coatings. *Science* **2007**, *318*, 426-430.
- (57) Yeroslavsky, G.; Girshevitz, O.; Foster-Frey, J.; Donovan, D. M.; Rahimipour, S. Antibacterial and Antibiofilm Surfaces through Polydopamine-Assisted Immobilization of Lysozyme as an Antibacterial Enzyme. *Langmuir* **2015**, *31*, 1064-1073.

- (58) Desbois, A. P.; Lang, S.; Gemmell, C. G.; Coote, P. J. Surface Disinfection Properties of the Combination of an Antimicrobial Peptide, Ranalexin, with an Endopeptidase, Lysostaphin, against Methicillin-Resistant Staphylococcus Aureus (Mrsa). *J. Appl. Microbiol.* **2010**, *108*, 723-730.
- (59) McDonald, J. C.; Whitesides, G. M. Poly (Dimethylsiloxane) as a Material for Fabricating Microfluidic Devices. *Acc. Chem. Res.* **2002**, *35*, 491-499.
- (60) Quake, S. R.; Scherer, A. From Micro-to Nanofabrication with Soft Materials. *Science* **2000**, *290*, 1536-1540.
- (61) Whitesides, G. M.; Ostuni, E.; Takayama, S.; Jiang, X.; Ingber, D. E. Soft Lithography in Biology and Biochemistry. *Annu. Rev. Biomed. Eng.* **2001**, *3*, 335-373.
- (62) Sui, G.; Wang, J.; Lee, C.-C.; Lu, W.; Lee, S. P.; Leyton, J. V.; Wu, A. M.; Tseng, H.-R. Solution-Phase Surface Modification in Intact Poly (Dimethylsiloxane) Microfluidic Channels. *Anal. Chem.* **2006**, *78*, 5543-5551.
- (63) Makamba, H.; Kim, J. H.; Lim, K.; Park, N.; Hahn, J. H. Surface Modification of Poly (Dimethylsiloxane) Microchannels. *Electrophoresis* **2003**, *24*, 3607-3619.
- (64) Goncalves, S.; Leirós, A.; Van Kooten, T.; Dourado, F.; Rodrigues, L. R. Physicochemical and Biological Evaluation of Poly (Ethylene Glycol) Methacrylate Grafted onto Poly (Dimethyl Siloxane) Surfaces for Prosthetic Devices. *Colloids Surf. B. Biointerfaces* **2013**, *109*, 228-235.



**Scheme 1** SARA SI-ATRP for coating with various antibacterial film formulations

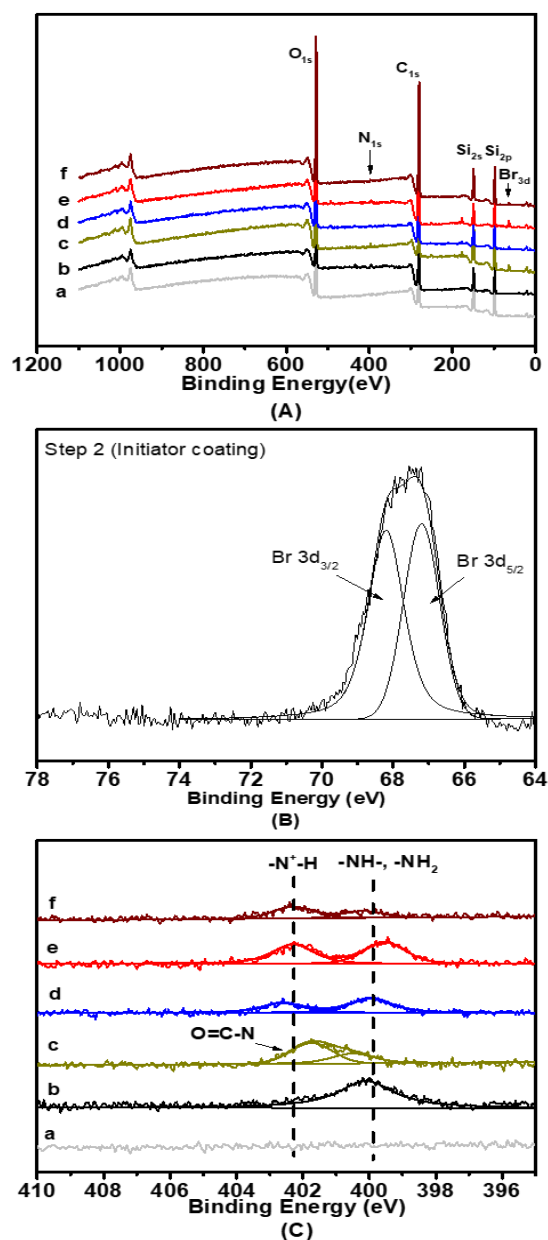


**Figure 1** X-ray photoelectron spectroscopy (XPS) (A) wide scan of (a) pristine PDMS catheter, (b) PDMS/PDA coating (Step 2), (c) BiBB/PDA/PDMS, (d) coating 1, (e) coating 2, (f) coating 3; (B) Br<sub>3d</sub> core level of BiBB/PDA/PDMS coating (Step 2); (C) N<sub>1s</sub> core level of (a) pristine PDMS catheter, (b) PDMS/PDA coating (Step 2), (c) BiBB/PDA/PDMS, (d) coating 1, (e) coating 2, (f) coating 3.

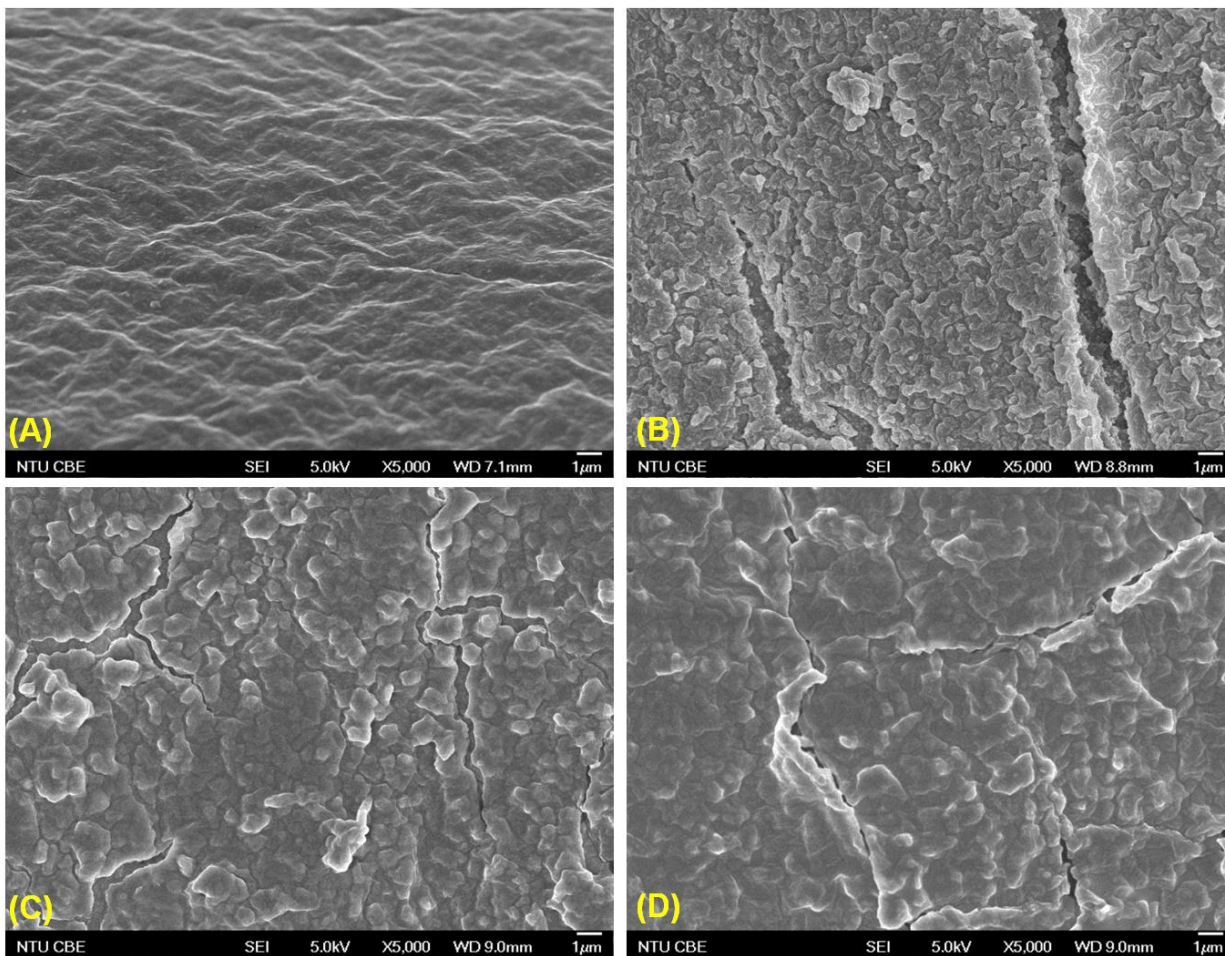


**Figure 2** FE-SEM of (A) pristine PDMS catheter, (B) coating 1, (C) coating 2 and (D) coating 3.

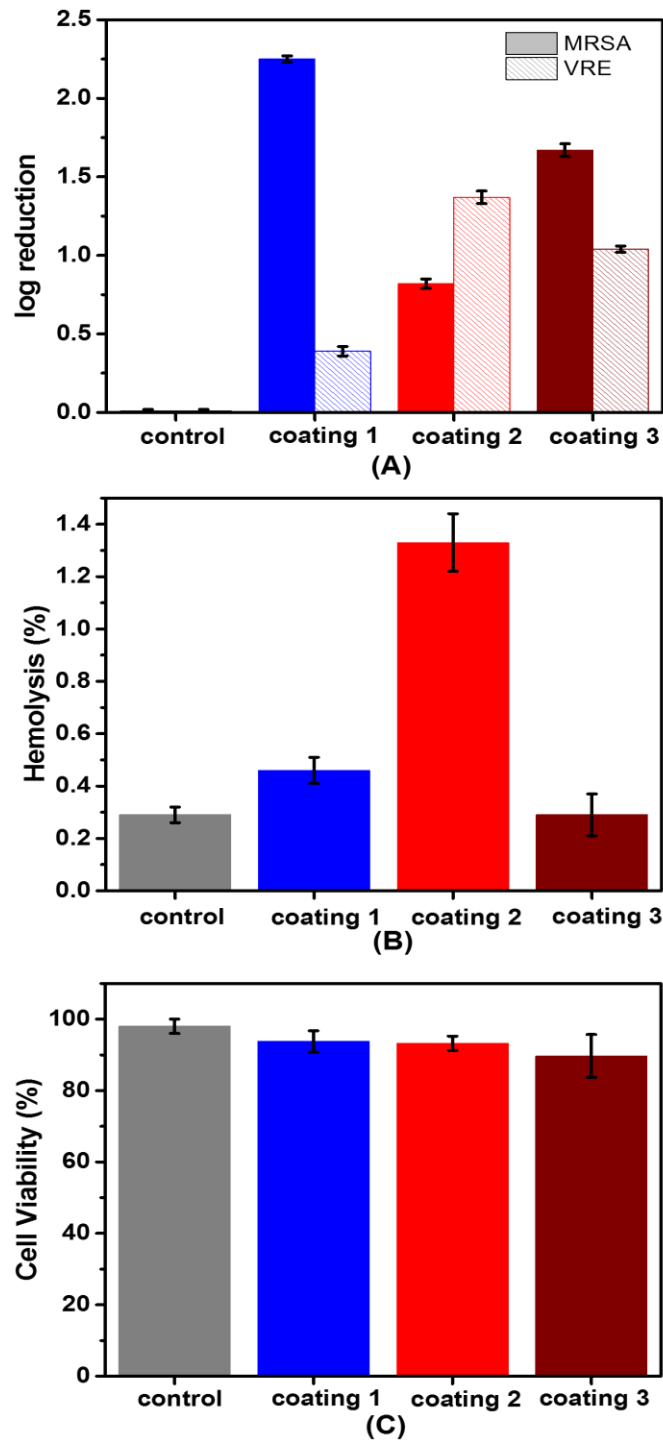
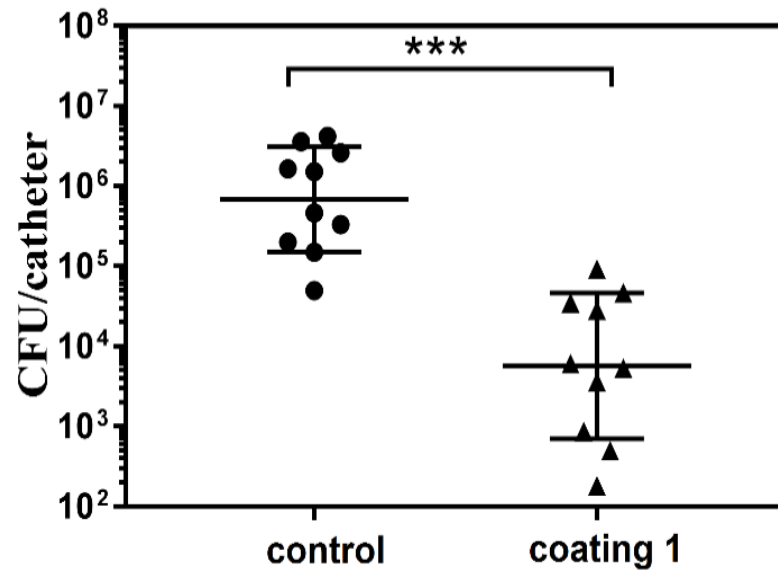
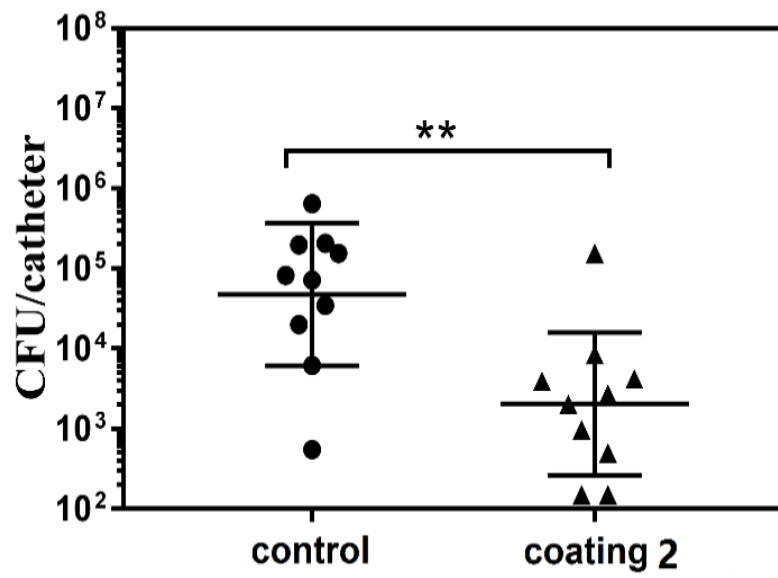


**Figure 3** (A) Viable surface colonies of *Ef.V583* and MRSA BAA40; (B) Hemolysis; (C) MTT assay of the cellular viability.



(A)



(B)

**Figure 4** CFU quantification from catheters in vivo (A) coating 1 for MRSA and (B) coating 2 for VRE.

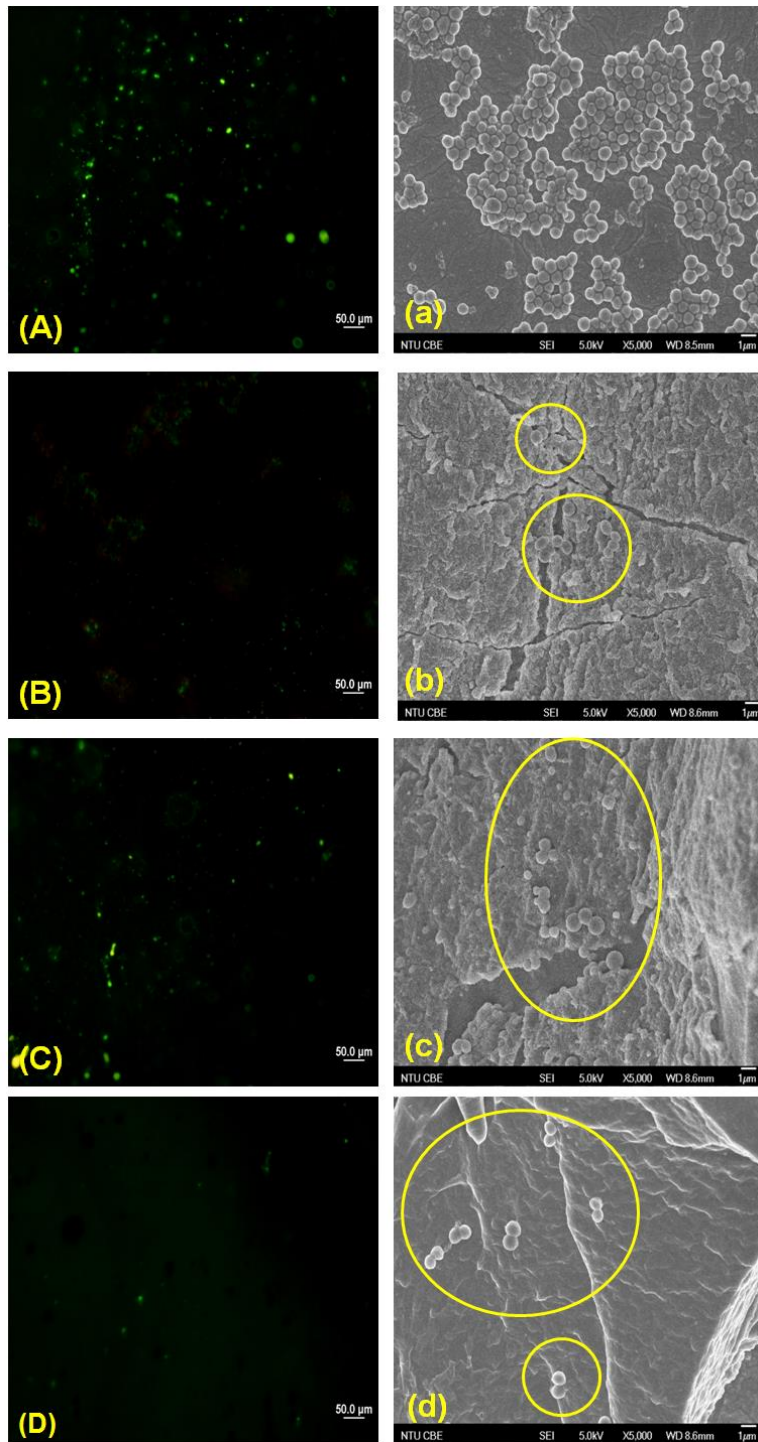


**Figure 5** Green fluorescence and FE-SEM images of MRSA on (A, a) pristine PDMS catheter; (B, b) coating 1; (C, c) coating 2 and (D, d) coating 3.

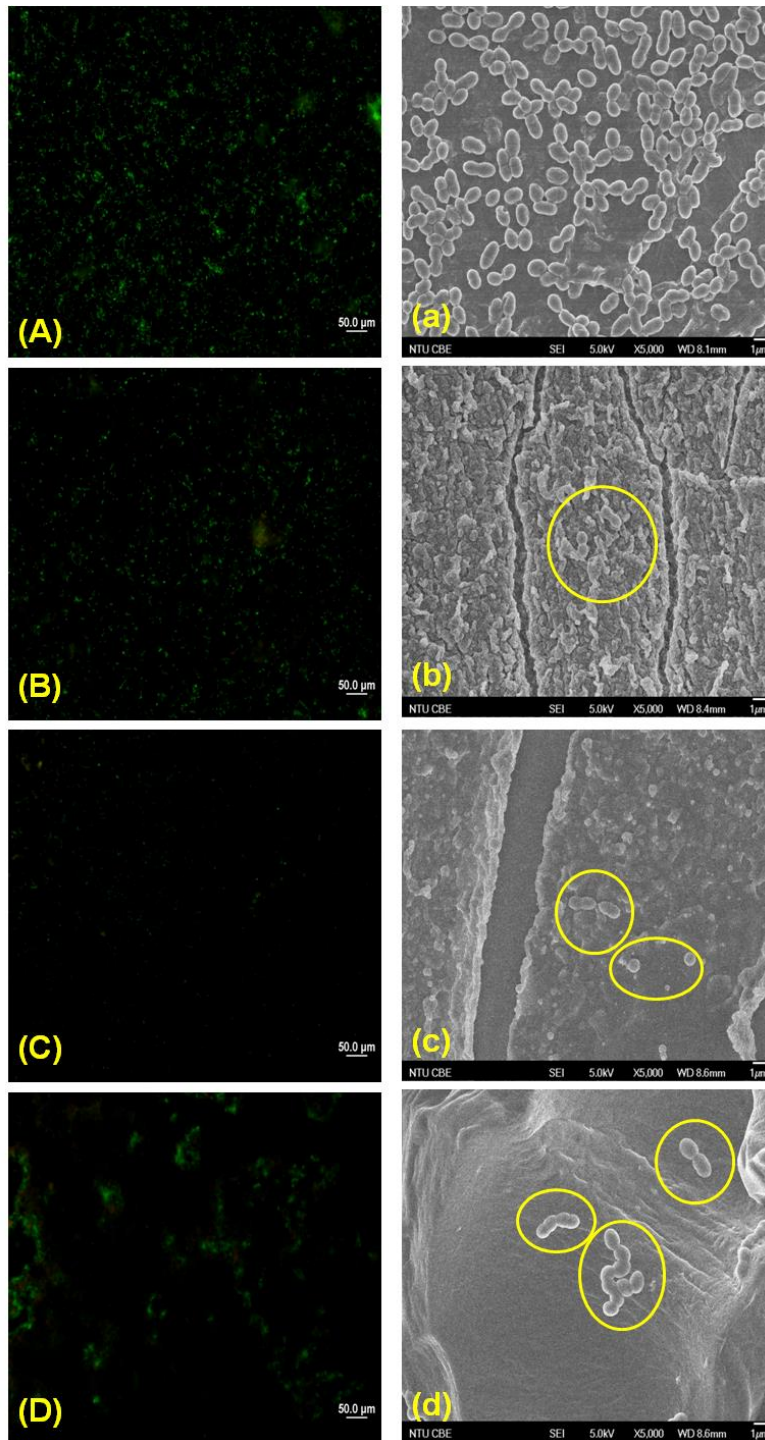


**Figure 6** Green fluorescence and FE-SEM images of VRE on (A, a) pristine PDMS catheter; (B, b) coating 1, (C, c) coating 2 and (D, d) coating 3.

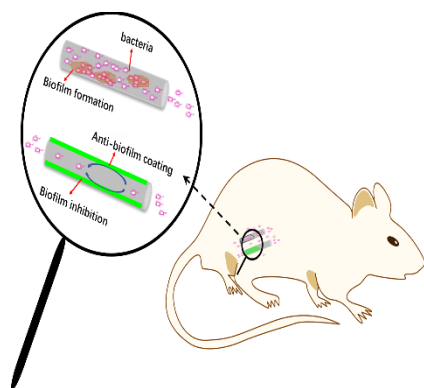
**Table 1** Coating formulations

Samples	AMPTMA	Q-PEI-MA	PEGDMA	CuBr <sub>2</sub> /PMDETA	Methanol/H <sub>2</sub> O
coating 1 (LD)	3.99 g		1.089 g	32.4mg/29.9uL	5 ml/5 ml
coating 1 (HD)	3.99 g		1.089 g	32.4mg/29.9uL	5 ml/5 ml
coating 1	3.99 g		1.089 g	32.4mg/29.9uL	5 ml/5 ml
coating 2	3.99 g	0.92 g	1.089 g	32.4mg/29.9uL	5 ml/5 ml
coating 3		0.92 g	1.089 g	32.4mg/29.9uL	5 ml/5 ml

**Table 2** Surface composition and water contact angle of coatings

Samples	XPS wide scan				C <sub>1s</sub> core-level scan					Contact angle [±3°]
	[Si]	[C]	[O]	[N]	[Br]	[C-H/C-C]	[C-N]	[C-O]	[-C=O]	
PDMS	1.00	1.24	1.58	-	-	1.000	-	0.144	-	109.3
Step 1	1.00	2.69	2.06	0.21	-	1.000	0.288	0.033	0.076	97.1
Step 2	1.00	2.30	2.58	0.26	0.83	1.000	0.068	0.038	0.044	91.4
Step 2 (LD)	1.00	2.68	3.06	0.27	0.58	1.000	0.176	0.041	0.011	95.6
Step 2 (HD)	1.00	2.37	2.63	0.20	0.94	1.000	0.218	0.056	0.046	93.3
coating 1 (LD)	1.00	2.23	2.67	0.28	0.32	1.000	0.285	0.321	0.068	64.9
coating 1 (HD)	1.00	2.57	2.93	0.39	0.09	1.000	0.393	0.088	0.0715	23.3
coating 1	1.00	2.18	2.49	0.31	0.39	1.000	0.307	0.289	0.058	32.7
coating 2	1.00	2.55	2.92	0.75	0.47	1.000	0.578	0.143	0.064	49.1
coating 3	1.00	2.04	2.25	0.29	0.20	1.000	0.283	0.316	0.060	96.6

## *In Vivo* Anti-Biofilm and Anti-Bacterial Non-Leachable Coating Thermally Polymerized on Cylindrical Catheter



The anti-bacterial and anti-biofilm non-leachable coatings on PDMS catheter were prepared by SARA SI-ATRP, which could against various MDR bacteria.

## Supporting Information

# *In Vivo* Anti-Biofilm and Anti-Bacterial Non-Leachable Coating Thermally Polymerized on Cylindrical Catheter

Chao Zhou,<sup>‡1,2</sup> Yang Wu,<sup>‡1,2</sup> Kishore Reddy Venkata Thappeta,<sup>‡3</sup> Jo Thy Lachumy Subramanian,<sup>1,2</sup> Dicky Pranantyo,<sup>4</sup> ET Kang,<sup>4</sup> Hongwei Duan<sup>1,2</sup>, Kimberly Kline,<sup>2,3</sup> Mary B. Chan-Park<sup>\*1,2</sup>

- <sup>1.</sup> *School of Chemical and Biomedical Engineering, Nanyang Technological University (NTU), 62 Nanyang Drive, Singapore 637459.*
- <sup>2.</sup> *NTU, Centre for Antimicrobial Bioengineering.*
- <sup>3.</sup> *Singapore Centre for Environmental Life Science Engineering (SCELSE), School of Biological Sciences, Nanyang Technological University, Singapore.*
- <sup>4.</sup> *National University of Singapore, Department of Chemical and Biomolecular Engineering, Singapore*

[\\*mbechan@ntu.edu.sg](mailto:mbechan@ntu.edu.sg)

<sup>‡</sup> *These authors contribute equally.*

**Table S1** zeta potential & MIC of monomers

Monomers	Zeta potential (mV)	Minimal inhibitory concentration (MIC)				
		E. coli 8739	MRSA BAA40	P. aeruginosa 01	S. aureus 29213	Ef. V583
Quaternized PEI-MA	36.2	>512	>512	>512	>512	>512

**Table S2** *In vitro* log reduction data and MTT assay of coating 1 (LD), coating 1 (HD), coating 1 (AC), and coating 2 (AC)

Samples	Log reduction		MTT
	MRSA	VRE	
coating 1 (LD)	1.10±0.01		91.12%
coating 1 (HD)	1.77±0.01		92.08%
coating 1 (AC)	1.85±0.02		91.15%
coating 2 (AC)		1.36±0.01	90.59%

**Table S3** Surface Zeta potential of coatings

Samples (Flat film)	Log reduction	Contact angle [±3°]	Surface Zeta Potential (mV)
	MRSA		
coating 1 (LD)	1.05±0.01	65.1	5.7±0.3
coating 1 (HD)	1.70±0.03	30.0	19.4±0.1
coating 1	1.85±0.02	34.1	17.1±0.5
coating 2	0.78±0.01	53.2	28.3±0.3
coating 3	1.45±0.03	99.1	13.5±0.4

**Table S4** *In vivo* data of coating 1 for MRSA

<b>Samples</b>	<b>In vivo CAUTI with <i>MRSA BAA40</i></b>					<b>Mean</b>	<b>Geometric mean</b>	<b>Log reduction</b>
<b>control</b>	2.63E+06	4.17E+05	3.68E+06	4.83E+05	1.20E+06	1.68E+06	1.19E+06	
<b>coating 1</b>	8.16E+03	6.67E+03	1.13E+04	5.00E+04		1.90E+04	1.33E+04	1.95

**Table S5** *In vivo* data of coating 3 for VRE

<b>Samples</b>	<b>In vivo CAUTI with <i>E.faecalis</i> V583</b>					<b>Mean</b>	<b>Geometric mean</b>	<b>Log reduction</b>
<b>control</b>	5.50E+02	2.07E+05	6.50E+05	6.20E+03	7.17E+04	1.87E+05	3.19E+04	
<b>coating 2</b>	5.00E+02	9.67E+02	4.22E+03	3.90E+03	2.03E+03	2.32E+03	1.75E+03	1.26



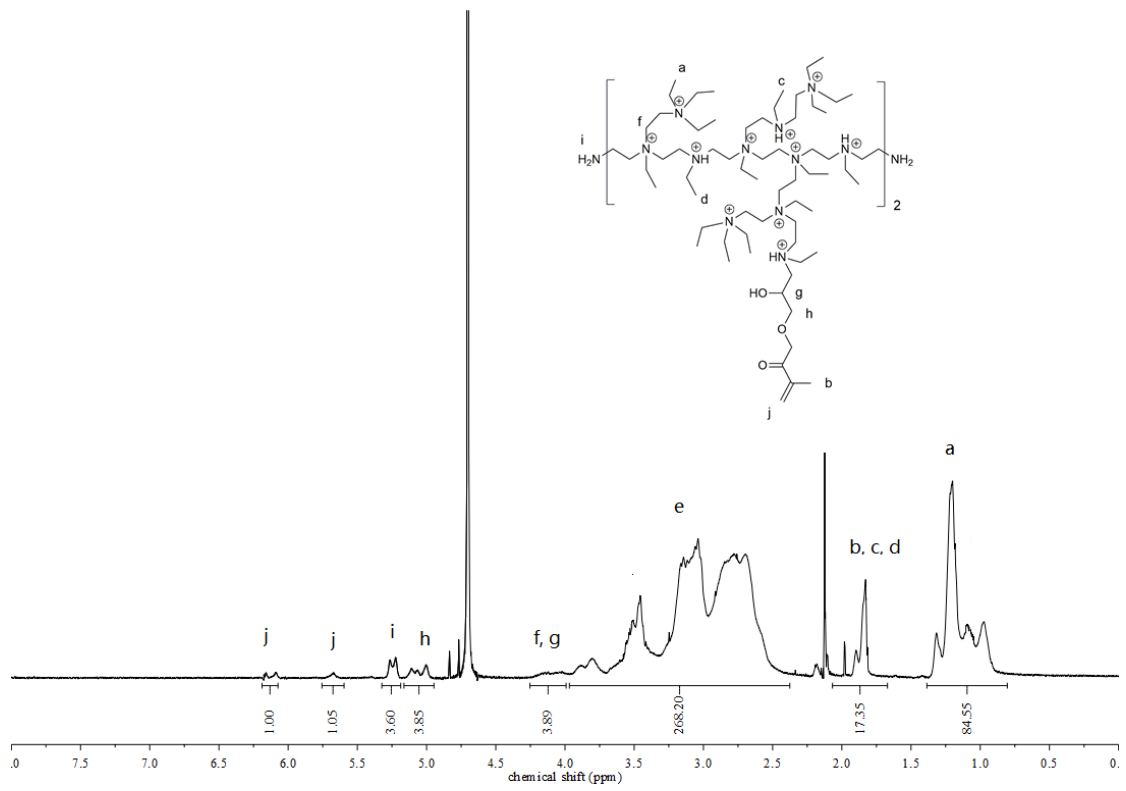


**Figure S1** <sup>1</sup>H NMR of Q-PEI-MA

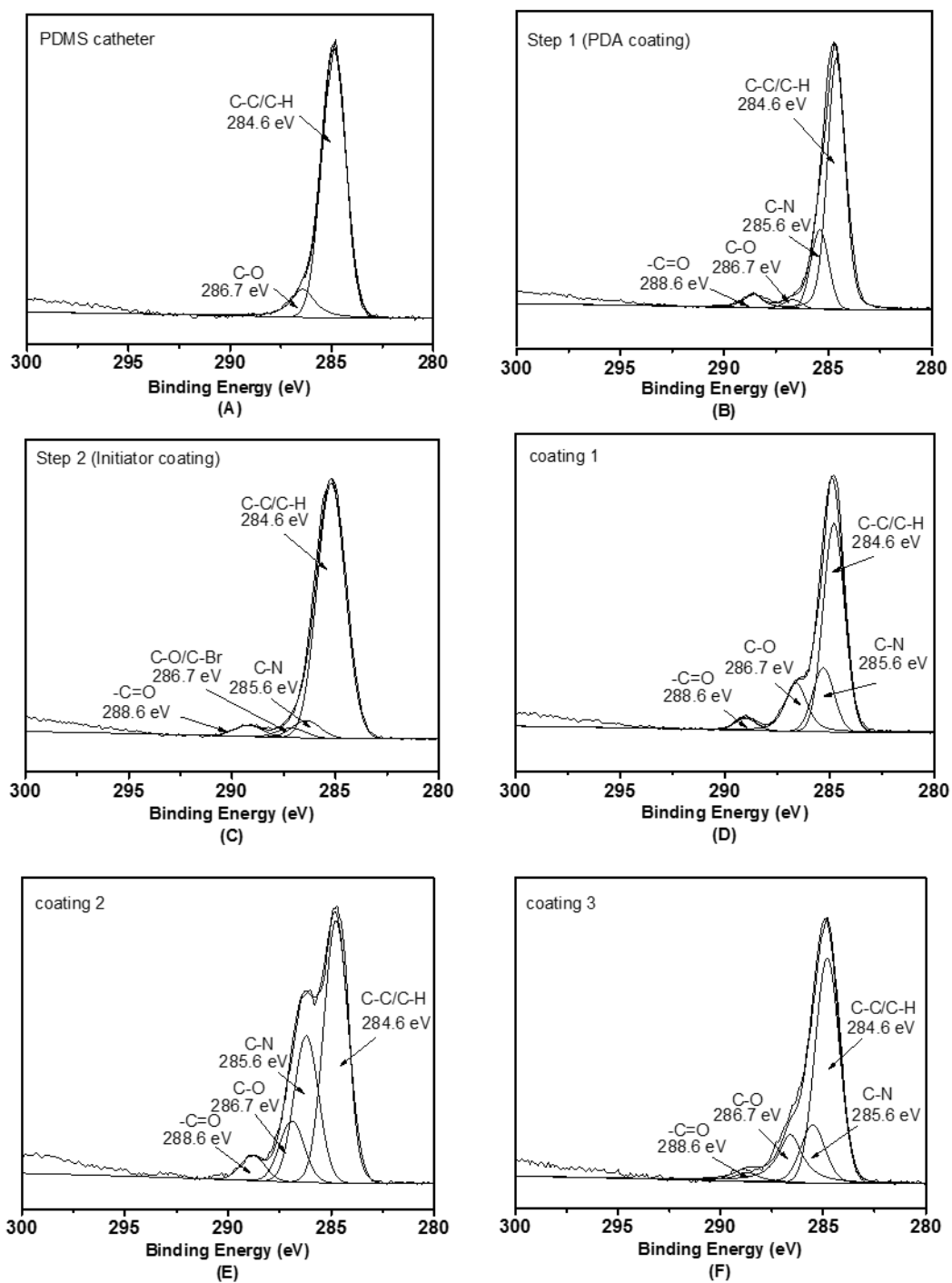


**Figure S2** XPS of  $C_{1s}$  core level spectra: (A) pristine PDMS catheter, (B) PDA/PDMS coating (Step 1), (C) BiBB/PDA/PDMS (Step 2), (D) coating 1, (E) coating 2, (F) coating 3.

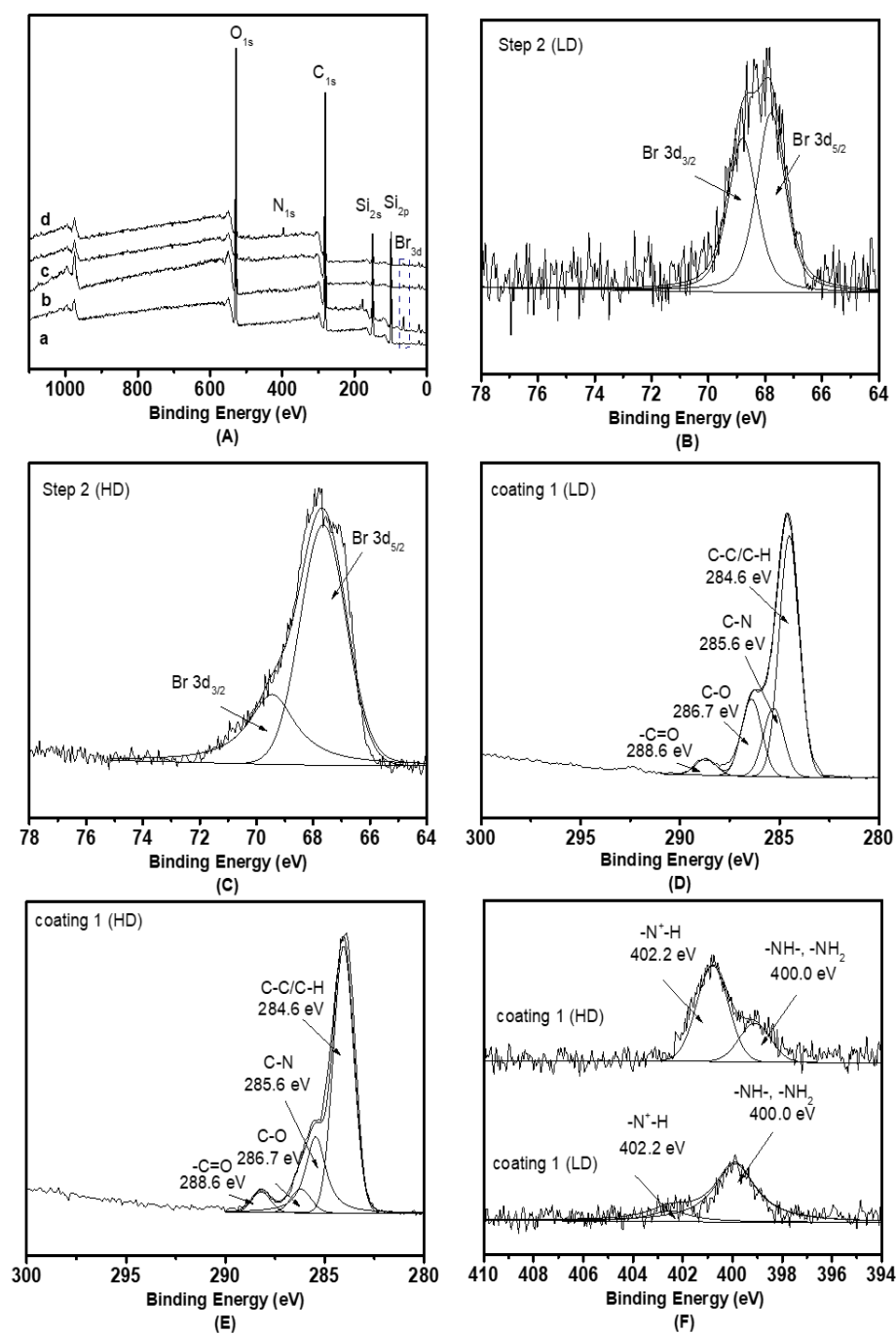


**Figure S3** X-ray photoelectron spectroscopy (XPS) (A) wide scan of a: Step 2 (LD), b: Step 2 (HD), c: coating 1 (LD), d: coating 1 (HD); (B)  $Br_{3d}$  core level spectra of Step 2 (LD); (C)  $Br_{3d}$  core level spectra of Step 2 (HD); (D)  $C_{1s}$  core level spectra of coating 1 (LD); (E)  $C_{1s}$  core level spectra of coating 1 (HD); (F)  $N_{1s}$  core level spectra of coating 1 (LD) and coating 1 (HD).

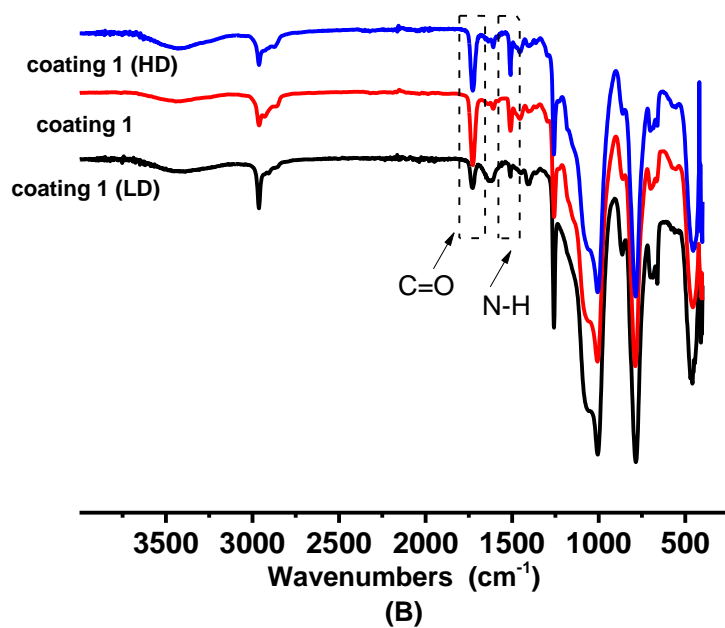
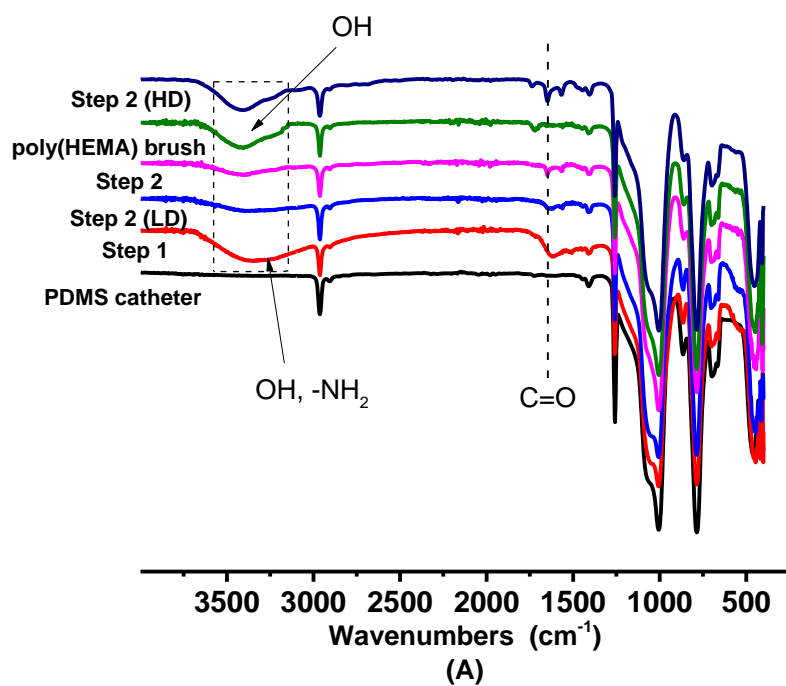


**Figure S4** FTIR-ATR of (A) surface PDA coating (Step 1), poly(HEMA) brush coating and surface after BiBB grafting with normal (Step 2), low (Step 2 (LD)) and high (Step 2 (HD)) BiBB density; (B) coating 1 (LD), coating 1, and coating 1 (HD).

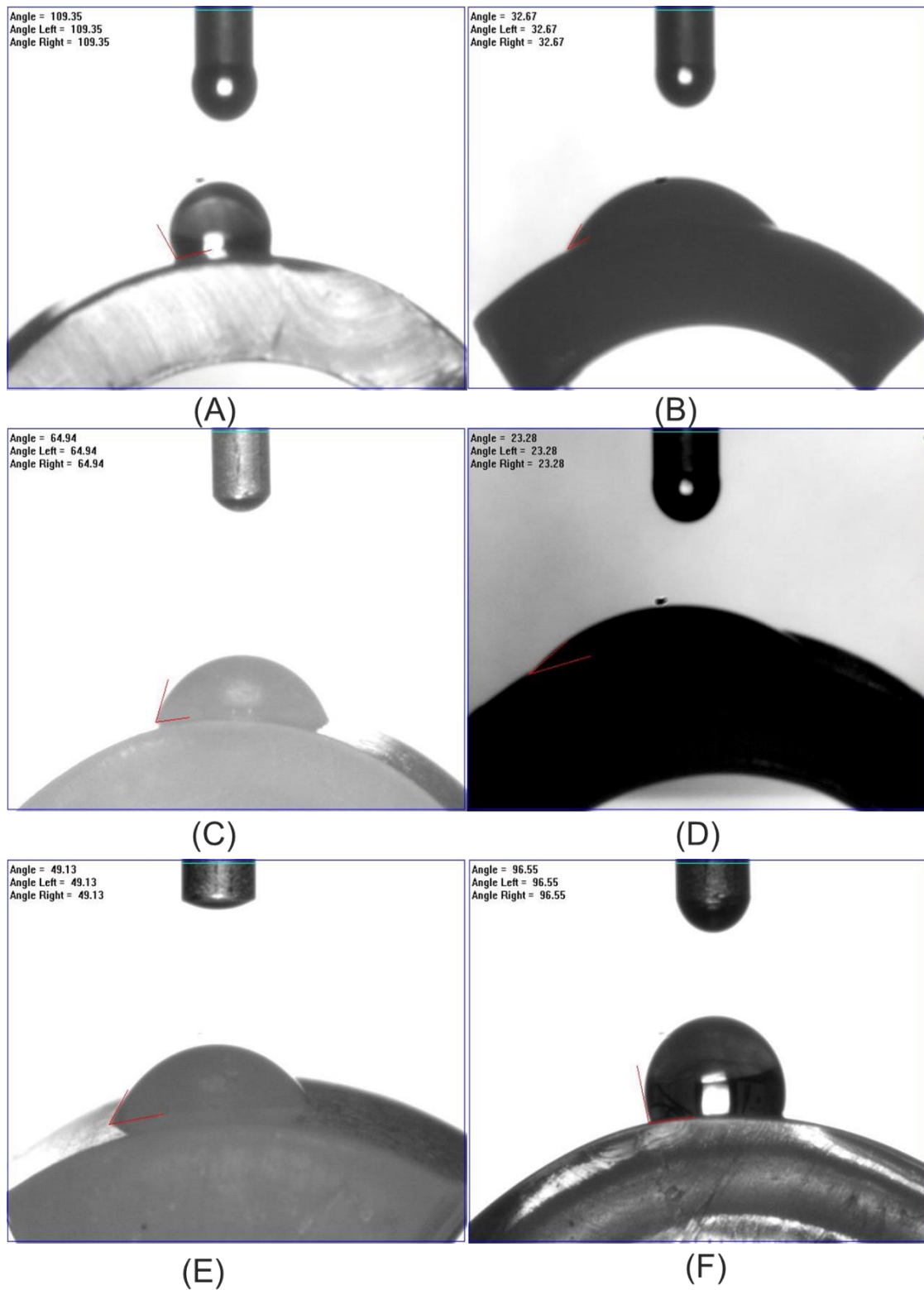


**Figure S5** Contact angle of (A) pristine PDMS catheter, (B) coating 1, (C) coating 1 (LD), (D) coating 1 (HD), (E) coating 2, (F) coating 3.

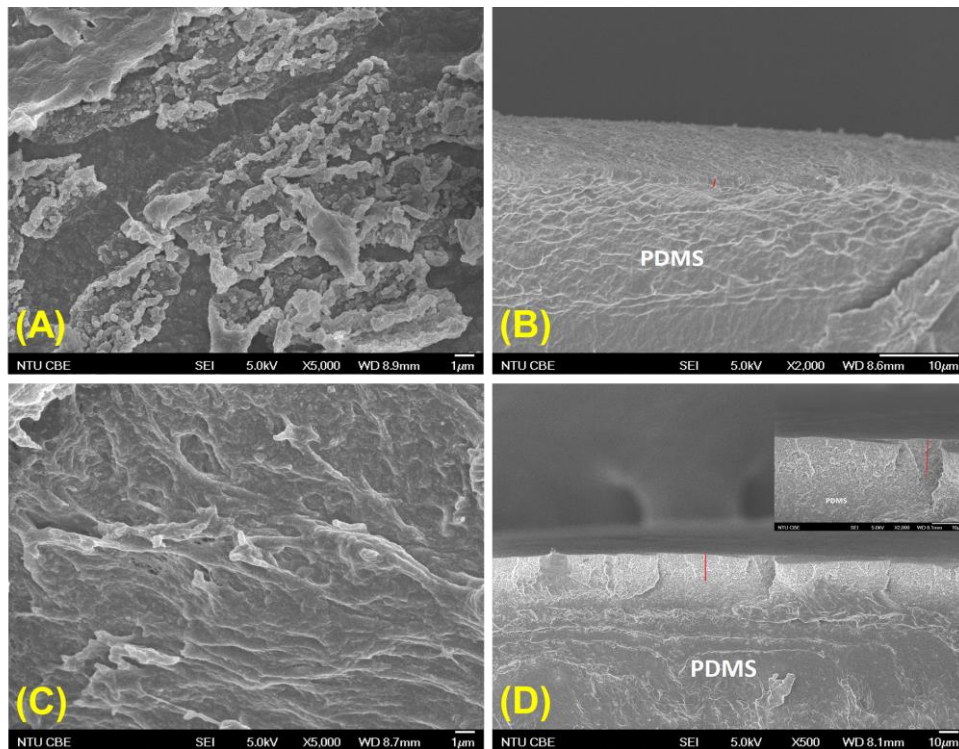


**Figure S6** FE-SEM (A) top view of coating 1 (LD); (B) cross section view of coating 1 (LD); (C) top view of coating 1 (HD); (D) cross section view of coating 1 (HD), the red lines indicate the coating depth.

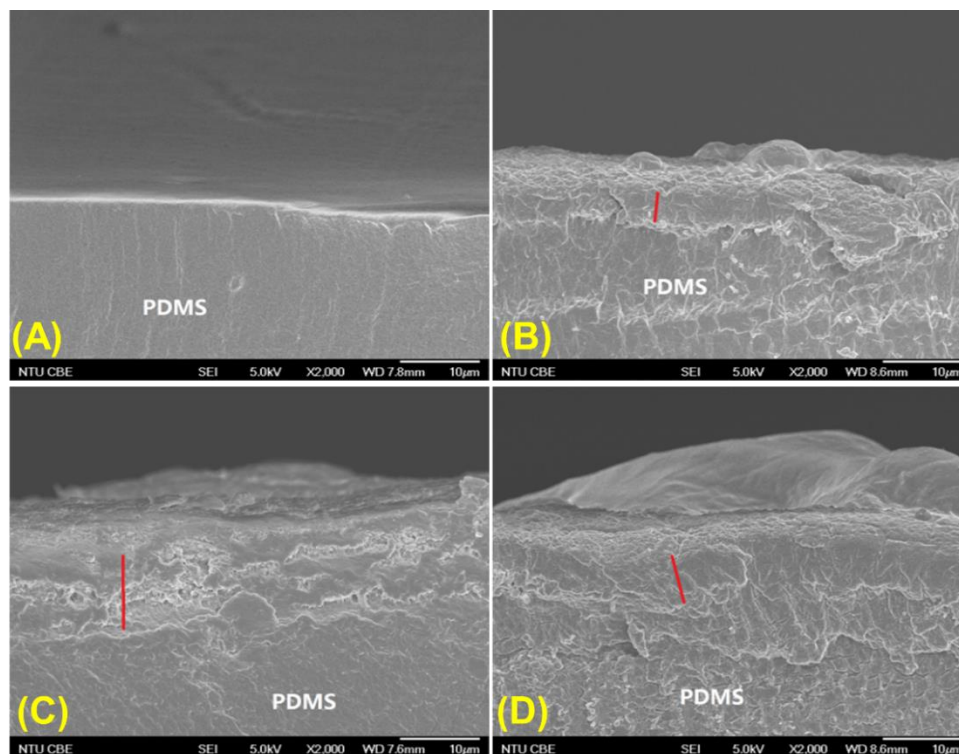


**Figure S7** FE-SEM cross section views of (A) pristine PDMS catheter, (B) coating 1, (C) coating 2, (D) coating 3. The red lines indicate the coating depth, which varies from about 2.5 to about 9.5 microns across the various samples.

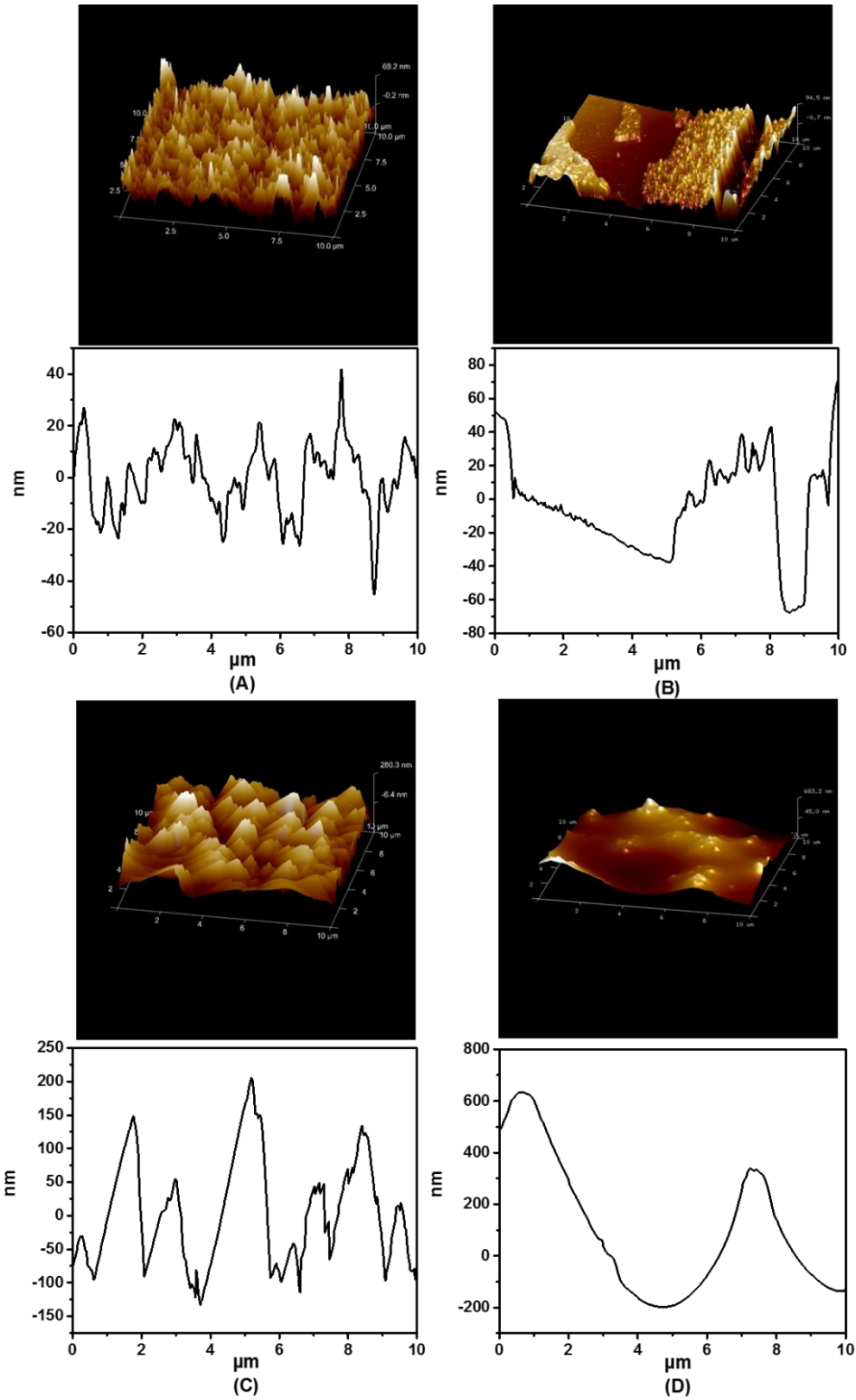


**Figure S8** AFM of (A) pristine PDMS catheter, (B) PDA on PDMS coating, (C) coating 1 (LD), (D) coating 1 (HD).

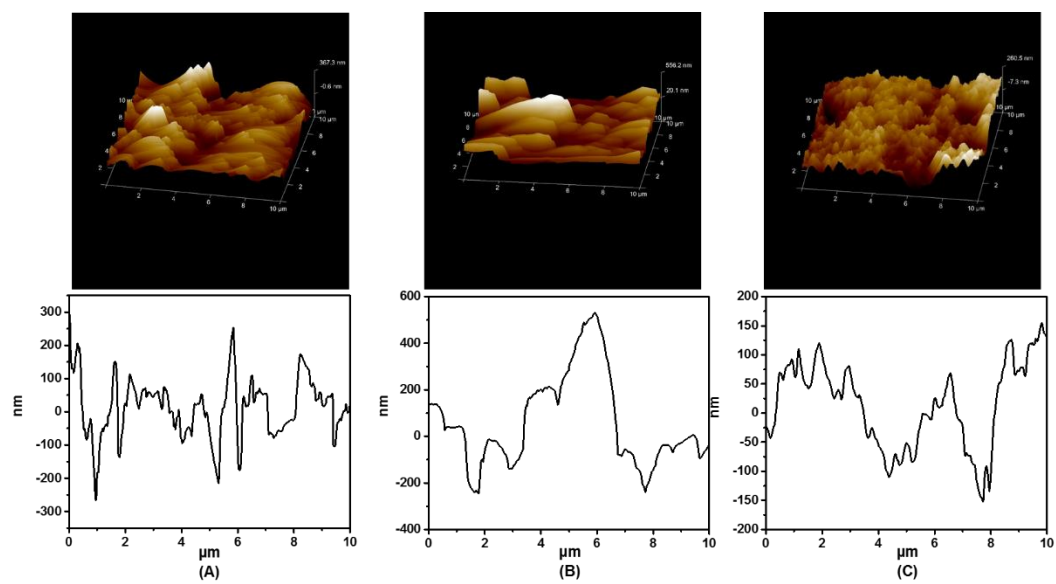


**Figure S9** AFM of (A) coating 1, (B) coating 2, (C) coating 3.

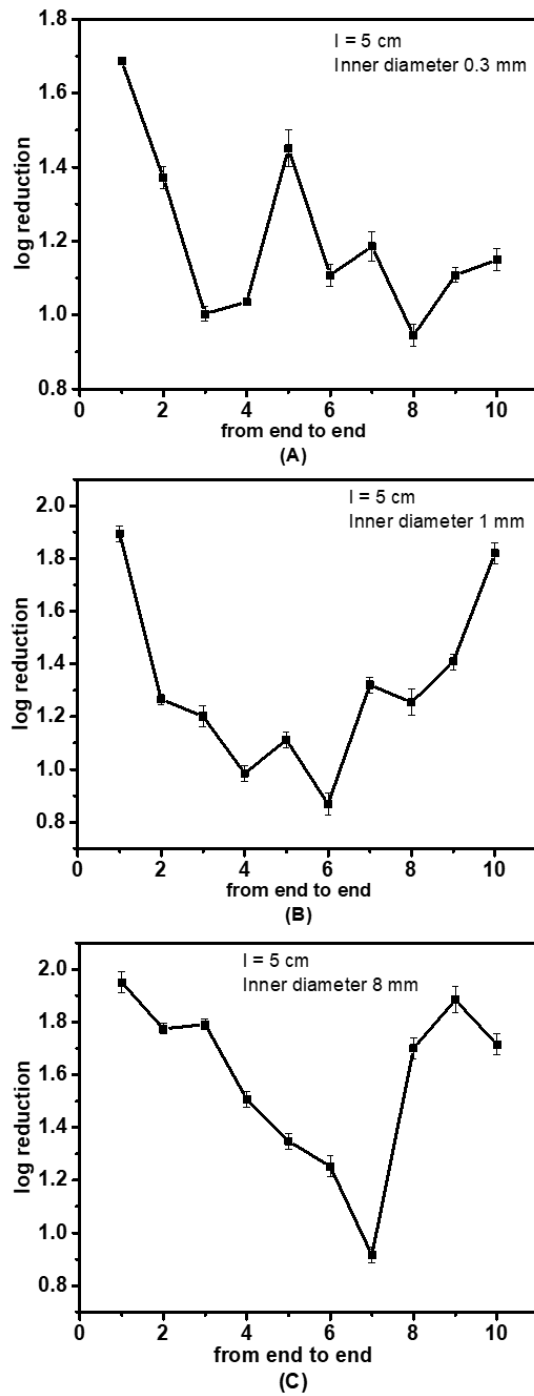


**Figure S10** CFU count *in vitro* of coating 1 onto different inner diameters of long catheter ( $l=5$  cm) for MRSA (A) inner diameter 0.3mm, (B) inner diameter 1 mm and (C) inner diameter 8 mm.